Fleet availability analysis and prediction for shared e-scooters: An energy perspective

Transportation Research Part D 136 (2024) 104425

Contents lists available at ScienceDirect

Transportation Research Part D

journal homepage: www.elsevier.com/locate/trd

Fleet availability analysis and prediction for shared e-scooters: An energy perspective

Jiahui Zhao [a], Jiaming Wu [b,*], Sunney Fotedar [b], Zhibin Li [a], Pan Liu [a]

[a] School of Transportation, Southeast University, Nanjing, China
[b] Architecture and Civil Engineering, Chalmers University of Technology, Gothenburg, Sweden

ARTICLE INFO

Keywords:
Micro-mobility
Fleet availability
OD prediction
Energy consumption

ABSTRACT

E-scooters have become a prevalent mode of transportation in many cities. The availability of e-scooters is a crucial indicator of service quality but has not been sufficiently investigated. We propose a two-stage method for fleet availability analysis and prediction, considering stochastic demand and a new energy perspective. First, we developed a SpatioTemporalAttentionNet (STAN) model to predict trip OD. Second, we propose a Monte Carlo-based algorithm to match demand with existing e-scooters across spatiotemporal and energy dimensions. We conduct case studies using real-world data from Gothenburg, Sweden. The results indicate an average unavailability rate of 6.71%, nearly doubling that of the benchmark group, which uses a 20% SoC threshold for determining availability. This rate is significant considering the large fleet size and highlights the need to incorporate battery levels into fleet management. We further investigate the multifaceted impacts of land use and walking distance on availability dynamics.

1. Introduction

Dockless shared electric scooters (e-scooters) have become a popular mode of short-distance travel in urban areas. Compared to conventional shared bicycles, e-scooters are battery-powered, providing both convenience and enjoyment. Soon after their debut in 2017, e-scooters rapidly dominated the micro-mobility market (Li et al., 2022). As of 2023, the global e-scooter user base has surpassed 90 million, with the United States and Europe as the primary markets. This figure is projected to reach 133 million by 2027 (Statista, 2023).

Along with their growing popularity, serious concerns have been raised, including extensive energy consumption and urban space usage, leading to regulatory clampdowns (Fearnley, 2020). For instance, Paris has enacted strict regulations to restrict e-scooter riding exclusively to cycle lanes (Roberts, 2023), and Stockholm has introduced a cap of 1500 scooters per operator (Anderson, 2022). These are signs that cities demand well-managed mobility services and changes in practices from operators. In response, companies are compelled to enhance their safety measures, operations, and even vehicle designs. Experience is summarized in a memo of best industry practices, recommended jointly by five major operators (Dott, Lime, Superpedestrian, Tier, and Voi) in Europe (May, 2023). After several years of development, it became common practice for cities to issue a limited number of permits, and companies compete for positions in tenders. This business model underscores the importance of efficient fleet management, which was crucial for winning tenders.

* Correspondence to: Department of Architecture and Civil Engineering, Chalmers University of Technology, Room 440, Sven Hultins gata 6 SE-412 96, Gothenburg, Sweden.
E-mail addresses: jiahuizhao@seu.edu.cn (J. Zhao), jiaming.wu@chalmers.se (J. Wu), sunney@chalmers.se (S. Fotedar), lizhibin@seu.edu.cn (Z. Li), liupan@seu.edu.cn (P. Liu).
URL: https://research.chalmers.se/en/person/jiwu (J. Wu).

https://doi.org/10.1016/j.trd.2024.104425
Received 7 May 2024; Received in revised form 12 September 2024; Accepted 12 September 2024
Available online 24 September 2024

Meanwhile, e-scooters have sparked growing interest in the research community. Existing studies primarily focus on understanding travel behavior changes induced by e-scooters (Zakhem and Smith-Colin, 2021; Orvin et al., 2022; Li et al., 2022) and operational management problems (Ayyildiz, 2022; Giordano and Chow, 2024). Despite significant efforts, a notable gap remains largely overlooked: how to evaluate the operational performance of e-scooters. This was crucial for cities to gain an evidence-based understanding of service quality and for companies to direct their fleet management practices. Currently, this remained an unattended area, as conventional metrics like the level of service have not yet been defined for e-scooters (Kazemzadeh and Sprei, 2022). This research addresses this issue by proposing a method for fleet availability analysis and prediction, an intuitive approach to examine demand fulfillment, and an innovative perspective considering battery energy.

Fleet availability in traditional shared mobility systems, such as bikes, is determined exclusively by the locations of the vehicles (Reck et al., 2022). Availability is assured as long as users can find nearby vehicles. However, this does not apply to e-scooters. An e-scooter is effectively available only when it is nearby and has sufficient battery power to complete the desired trip. Therefore, analyzing e-scooter availability requires considering both demand and energy metrics. In this paper, we consider **Availability** as a performance metric for a pre-determined traffic analysis zone in a specific time window. It is defined as the ratio of e-scooters within a maximum walking distance and with sufficient battery levels for anticipated trips to the current number of vehicles in the zone. Mathematically, it can be expressed as:

$$A_{i,t+1} = \frac{n_{i,t}(d_{t+1})}{N_{i,t}} \tag{1}$$

where $A_{i,t+1}$ denotes the predicted availability for zone i at time $t+1$; $n_{i,t}(d_{t+1})$ denotes the number of e-scooters within maximum walking distance and, at the same time, currently having sufficient battery level for the anticipated demand d_{t+1} of the next time step; $N_{i,t}$ denotes the total number of vehicles in zone i at time t. In practice, a predictive estimation of fleet availability is more meaningful, as it enables proactive management. For instance, operators charge e-scooters daily. Although all prevailing e-scooters are designed for fast onsite battery swapping, charging activities remain time-consuming due to the large fleet size. Data from major cities in Sweden indicate that it often takes at least four hours to charge only part of the fleet (Wang et al., 2021). Therefore, starting to charge when the availability level has already dropped below the desired level was too late.

Despite its significance, predicting fleet availability is challenging primarily due to its dynamic nature. Due to their compact and lightweight design, e-scooter systems are mostly operated without docking stations (Engdahl et al., 2020). This introduces significant uncertainties in their geo-locations, as users can park them almost anywhere (Tuli et al., 2021). Moreover, the adequacy of the battery level depends on the trip length rather than the absolute value of the battery's State of Charge (SoC). An e-scooter with 30% SoC is sufficient for a 5-minute trip but not for a 30-minute trip. Consequently, relying solely on the prediction of area demand, as commonly done in previous studies (Jiao and Bai, 2020; Orvin et al., 2022), is not a reliable or accurate approach for predicting e-scooter availability.

To address these challenges, we evaluate and predict e-scooter fleet availability using a two-stage model. In the first stage, we conduct trip Origin-Destination (OD) predictions to forecast future spatiotemporal demand and the corresponding desired battery energy. The prediction is focused on small geographical zones, rather than conventional large traffic analysis zones, to capture short-distance travel characteristics and reduce errors in trip length estimation. In the second stage, we match the predictions with the existing e-scooters and their SoCs using a Monte Carlo algorithm. The contributions of this work are summarized as follows.

- To the best of our knowledge, this is the first study that integrates battery energy perspectives into fleet availability prediction for shared e-scooters.
- We propose a Monte Carlo-based approach to match predicted trips with existing e-scooters to determine spatiotemporal availability.
- We reveal the complex interactions between walking distance, land use, and e-scooter availability.

The remaining paper consists of five sections. The second section discusses relevant existing work for e-scooters. The third section presents an overview of the framework and methodology used in this work. The fourth section presents a case study based on data from the city of Gothenburg, Sweden. The last section concludes the paper with discussions and future work.

2. Literature review

In this section, we review prevailing studies in the field of e-scooter research, focusing on availability definition, demand prediction, operational management, and policies.

2.1. Availability definition

There is no literature that clearly defines the availability of e-scooters. Ashqar et al. (2017) and Almannaa et al. (2020) stated that traditional bike availability is the number of bikes or docks available at each bike station. However, Kabra et al. (2020) claimed that bike availability refers to the probability of encountering a bicycle. Due to the influence of battery levels, electric vehicle availability differs from traditional bike availability because the battery level also determines whether the vehicle can serve a trip. As stated by Ji et al. (2014), the service rate was used to evaluate the availability of the e-bike system, which was calculated as (the frequency of no e-bike + the frequency of no battery) / the total trip number. According to Zakhem and Smith-Colin (2021), Zhao et al. (2021) and Zhang and Zhao (2022), e-scooter availability was directly the number of e-scooter trip counts.

Table 1
The recent studies about micro-mobility demand prediction.

Papers	Type	OD	Weather	Time	Sparse Features	Energy
Song et al. (2023)	E-scooter	✓	✓	✓	✓	×
Lee et al. (2021)	E-scooter	×	×	×	×	×
Ham et al. (2021)	E-scooter	×	×	×	✓	×
Kim et al. (2022)	E-scooter	×	✓	✓	×	×
Phithakkitnukooon et al. (2021)	E-scooter	×	×	✓	×	×
He and Shin (2020)	E-scooter	×	×	✓	×	×
Fietz (2020)	E-scooter	×	✓	✓	×	×
Orvin et al. (2022)	E-scooter	×	✓	✓	×	×
Guidon et al. (2020)	E-bike	×	×	✓	✓	×
Butt et al. (2023)	E-bike	×	✓	✓	×	×
Jain et al. (2024)	E-two-wheelers	×	×	×	×	✓
Xu et al. (2018)	Bike	×	✓	✓	×	–
Yang et al. (2020)	Bike	✓	✓	✓	✓	–
Xu et al. (2020a)	Bike	×	×	×	×	–
Xu et al. (2020b)	Bike	×	✓	✓	✓	–
Sathishkumar et al. (2020)	Bike	×	×	×	✓	–
Liu et al. (2018)	Bike	✓	×	✓	✓	–

2.2. Demand prediction

Demand prediction is a fundamental aspect of transportation research, particularly in the field of shared micro-mobility. It serves as an input for operational optimization, providing proactive insights into forthcoming user needs and facilitating efficient vehicle re-balancing. The short-distance use of shared micro-mobility modes like bicycles and e-scooters is highly sensitive to factors such as weather and terrain, making demand predictions more challenging compared to other modes. In this sector, learning-based models have become popular and effective in demand predictions due to the large volume of available data.

Field data on e-scooter usage are inherently sparse and stochastic, requiring tailored configurations of learning models. In this context, Phithakkitnukooon et al. (2021) developed a demand prediction model for e-scooters that leverages a masking process and a weighted loss function. This method addressed the challenges associated with the sparse data commonly encountered in e-scooter usage analysis. Considering the stochastic demand, Saum et al. (2020) applied Box–Cox transformation, Seasonal ARIMA, and Autoregressive Conditional Heteroscedasticity models to predict e-scooter hourly demand. Foissaud et al. (2022) presented GCScoot, a dynamic flow distribution prediction model for urban e-scooter system reconfiguration, introducing a spatiotemporal graph capsule neural network. The model utilized real-world e-scooter mobility data to transform historical spatial distributions into flow graph structures, accurately predicting future e-scooter flows within reconfigured regions. This approach captured dynamic region-to-region correlations and contributed to optimizing e-scooter deployment (He and Shin, 2020). Ham et al. (2021) proposed the Encoder–Recurrent Neural Network–Decoder (ERD) framework to address the zero-inflation problem in demand prediction.

OD prediction, as an extension of demand prediction, offers a deeper understanding of user behavior and need distributions (Afandizadeh Zargari et al., 2021; Feng et al., 2022; Li et al., 2022; Karimpour et al., 2023). In this context, Merlin et al. (2021) developed Hurdle models for trip origins and destinations using data from Washington, DC. Their findings indicated that areas near tourist sites, hotels, and transit stops attract the most scooter-trip destinations, while the availability of e-scooters significantly influences trip origins. Song et al. (2023) proposed the Sparse Diffusion Convolutional Gated Recurrent Unit (SpDCGRU), which incorporates diffusion convolution layers into the Gated Recurrent Unit (GRU) model, enabling the simultaneous capture of spatiotemporal dependencies. Periodic and weather variables were found to have a positive effect on predicting both low and high demand for trip levels. E-scooter companies use OD distribution predictions to allocate resources efficiently and ensure that e-scooters are accessible when and where users need them.

In Table 1, we summarize recent studies in this field. We observe that these studies primarily focus on demand prediction, with particular attention given to the characteristics of data sparsity. However, there seems to be an oversight regarding the impact of battery levels on demand prediction for electric micro-mobility.

2.3. Operational management

Most operators use the SoC to indicate the remaining percentage of available battery capacity (Rechkemmer et al., 2017). When the SoC drops below a threshold, the e-scooter will be temporarily disabled and wait for a battery swap. In current practice, the threshold is usually set at 20% as a tradeoff between usability and battery degradation (Buchmann, 2003). Due to the relatively small battery capacity, battery-swapping tasks are intensive and performed daily or even several times a day. Considerable efforts have been devoted to improving charging strategies. Hollingsworth et al. (2019) and Liu et al. (2023) implemented optimal locations for charging stations and routes for fleet operation, resulting in reduced travel distance and emissions. Altintasi and Yalcinkaya (2022) introduced a GIS-based model to determine optimal locations for e-scooter charging stations. This model integrated the e-scooter system with existing public transportation systems and Points of Interest (POI). The charging stations received a suitability index of 1 if within walking distance of 400 to 800 m (Nacto Bike Share, 2015); otherwise, they were rated 0. Leurent (2022) evaluated

various SoC threshold values and their impact on systemic revenue generated by swappable batteries. Osorio et al. (2021) noted the importance of SoC in optimizing e-scooter distribution and rebalancing. They proposed charging strategies, such as in-route charging, to enhance the SoC of e-scooters. These strategies allow for quick battery swaps for e-scooters during rebalancing operations while in transit. Giordano and Chow (2024) introduced an innovative non-rooted maximum weighted connected subgraph model to enhance fleet allocation and meet demand responsively across contiguous service regions. Such models can guide operators in reallocating e-scooters to charging facilities before they become unavailable due to low SoC, thus maximizing e-scooter availability for potential users.

2.4. Regulations and tenders

To oversee the operations of e-scooters and avoid repeating the failures experienced by conventional shared bike systems, cities have adopted various approaches for regulating e-scooter fleets. Some cities have set limits on the number of permissible operators for e-scooter fleets. For instance, Milan has set a cap of 6000 e-scooters in total, whereas Rome has established a maximum fleet size of 14,500 e-scooters (Iolov, 2022). Turin has set a limit of 500 e-scooters per operator without imposing a total fleet size restriction (Study in Torino, 2020). In Rome, operators must remove or reposition scooters that are parked irregularly within six hours of being reported (Carrese et al., 2021). This regulation aims primarily to maintain the accessibility of sidewalks. Raleigh has legislation prohibiting e-scooters from being left out on the streets at night. This means that all e-scooters, even fully charged ones, must be collected daily. This results in additional costs and affects the availability and accessibility of e-scooter fleets (Hollingsworth et al., 2019).

In many cases, e-scooter operators must compete in public tenders to obtain an operation permit. In tenders, companies must meet strict criteria, including built-in speed limits, vehicle design guidelines, safety measures, equitable distribution, parking management, and environmental accountability (Ding et al., 2019; Fearnley, 2020; Sareen et al., 2021; Makkawi Gassim, 2024; Ge et al., 2018). For example, in 2019, Italy implemented specific technical standards for the Understanding and planning shared micro-mobilitdesign of e-scooters. These standards include the absence of seats, a maximum engine power of 500 W, a top speed limit of 20 km/h (reduced to 6 km/h in pedestrian zones), and a compulsory red light at the back (Carrese et al., 2021). In Austin, private e-scooter providers often place their fleets on the busiest streets to maximize profits. However, this practice does not necessarily benefit those in economically disadvantaged communities. City transport departments have modified the profit-driven business model used by these companies to make e-scooter services more accessible and advantageous for everyone. By integrating an equity analysis into contracts with private providers, the city can ensure that e-scooter services support the mobility needs of economically disadvantaged populations (Bai and Jiao, 2021). As a result, operators are motivated to monitor municipal key performance indicators to assess customer satisfaction and ensure they are meeting business goals, particularly focusing on vehicle availability (Nadkarni, 2020).

In our review of company reports, we discovered insights into market research on vehicle availability. According to the findings from 6-t (6T Research Office, 2019), the primary obstacle for users was the scarcity of nearby vehicles, a challenge encountered by 59% of respondents. Additionally, 24% of respondents stopped attempting to rent e-scooters due to the lack of nearby options. Furthermore, to increase their chances of finding an available scooter, 27% of users registered on multiple e-scooter applications, seeking one within a convenient walking distance. The Department for Transport in England also highlighted the significance of accessible e-scooters in their analysis (Department for Transport, 2022), emphasizing users' preference for scooters that were readily available near their living areas and within specific zones. Several surveys suggested that availability improved and usage increased when fleet sizes expanded and more parking areas were introduced, simplifying the process of locating e-scooters. Thus, improving accessibility was identified as a critical factor in boosting e-scooter usage based on the gathered data.

A number of studies also cover topics such as safety analysis (Ma et al., 2021; Drimlová et al., 2024), spatial and temporal usage patterns (Liu et al., 2019), user attitudes and engagement (Nikiforiadis et al., 2021; Askari et al., 2024), factors influencing usage (Hosseinzadeh et al., 2021; Wang et al., 2020a), and their impact on other modes of transportation (Guo et al., 2023; Yan et al., 2023; Jin and Sui, 2024). Interested reviewers are referred to the following review articles (Button et al., 2020; Zakhem and Smith-Colin, 2021; Sexton et al., 2023; Wang et al., 2023; Mitropoulos et al., 2023).

3. Methodology

This section presents a two-stage approach for predicting e-scooter fleet availability. In the first stage, we develop a state-of-the-art deep learning approach for short-term predictions of e-scooter trip ODs. The results include not only the predicted trips but also estimations of the battery energy to be consumed by those trips. In the second stage, we map existing e-scooters to the predictions using a Monte Carlo method to finalize the spatiotemporal fleet availability prediction.

3.1. Trip OD prediction

Following conventions in transport research, we divide the studied area into small Traffic Analysis Zones (TAZs) to facilitate modeling. Unlike automobiles and public transit, where trips span entire urban areas, e-scooters are predominantly used for short-distance travel. Considering the whole city for trip predictions will lead to a highly sparse OD matrix within the training dataset, potentially undermining the performance of learning algorithms. Therefore, we constrain the spatial range of OD predictions to a predefined rectangular zone near each trip's starting point, as illustrated in Fig. 1. Based on these insights, we adopted square grids

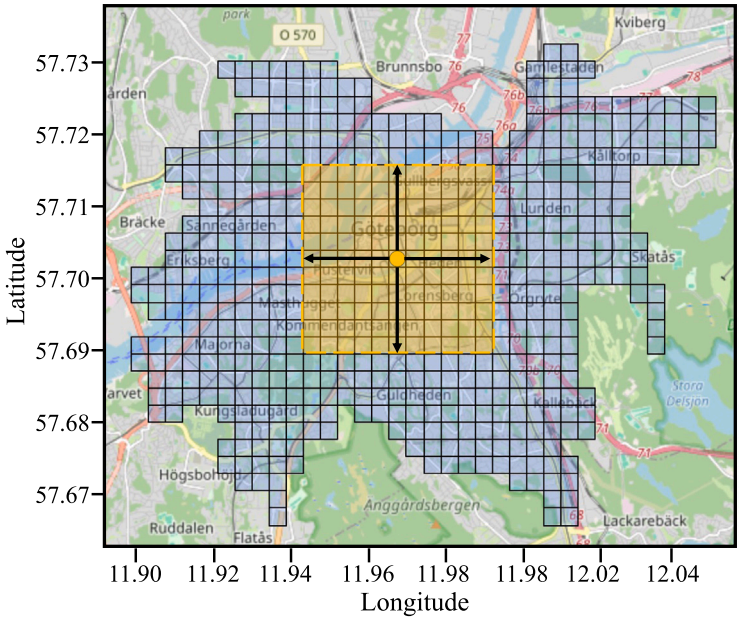

Fig. 1. The studied area in Gothenburg city.

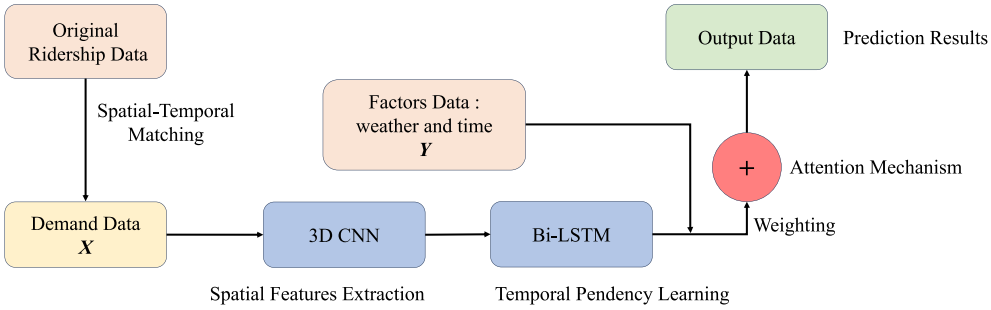

Fig. 2. The architecture of STAN.

to standardize TAZ shapes for predictive purposes. This approach aligns with techniques used in Zeng et al. (2021) and Yang et al. (2022) for demand forecasting and traffic analysis.

To tackle the e-scooter OD prediction problem, we propose a SpatioTemporalAttentionNet (STAN) model, comprising three integral modules: spatial, temporal, and attention modules, as shown in Fig. 2. The spatial module is designed to capture the spatial dependencies among different TAZs using a Three-dimensional Convolutional Neural Network (3D CNN). Temporal dependencies are captured through a Bidirectional Long Short-Term Memory (Bi-LSTM) Neural Network. Finally, we embed the attention mechanism to address regions with zero demand in certain time slots (such as off-peak hours). This combined approach enhances the understanding of how spatial interactions influence temporal dynamics, leading to more accurate e-scooter OD predictions. The STAN model stands out due to its advanced integration of spatial dependencies using 3D CNNs, effective handling of temporal sequences with Bi-LSTMs, and an adaptive attention mechanism. These features collectively enable the model to accurately predict e-scooter OD patterns, particularly in dynamic urban environments where demand varies spatially and temporally. Unlike traditional models, which may struggle to capture complex spatial and temporal relationships simultaneously, STAN's innovative approach explicitly models these interactions, resulting in more nuanced and precise predictions.

An overview of the input to STAN is illustrated in Fig. 3. The OD demand tensor is denoted by $D = [D^1, D^2, \dots, D^T]$, where D^t is the OD matrix and T represents the total number of time intervals (hourly discretization). Each $D^t \in \mathbb{R}_+^{m \times n}$ is a matrix denoted as

$$D^t = \begin{bmatrix} d^t_{1,1} & d^t_{1,2} & \dots & d^t_{1,n} \\ d^t_{2,1} & d^t_{2,2} & \dots & d^t_{2,n} \\ \vdots & \vdots & \ddots & \vdots \\ d^t_{m,1} & d^t_{m,2} & \dots & d^t_{m,n} \end{bmatrix},$$

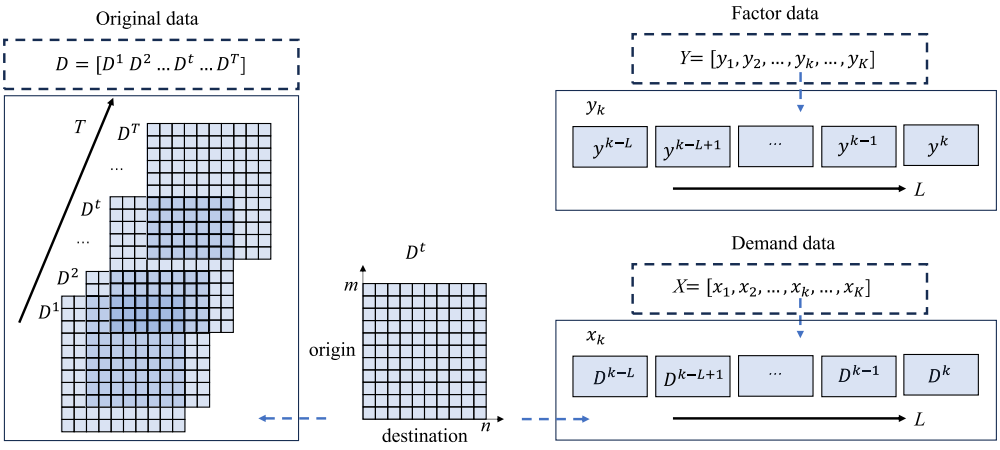

Fig. 3. The processing of input data.

where m represents the number of origin TAZs, and n represents the number of destination TAZs. Each element $d_{i,j}^t$ represents a trip from TAZ i to TAZ j at time interval t.

For a demand input sequence $X = [x_1, x_2, \dots, x_K]$, where $x_k = [D^{k-L}\ D^{k-L+1}\ \dots\ D^{k-1}\ D^k]$, $x_k \in \mathbb{R}_+^{m\times n\times L}$, k is the time interval, and L is the number of historical periods considered in each sequence. The factor sequences $Y = [y_1, y_2, \dots, y_K]$ include weather, holidays, and weekdays information, where $y_k \in \mathbb{R}^Q$ is the input feature vector at time step k, Q is the dimension of the feature vector, and K is the total number of time steps.

3.1.1. 3D CNN layer

The 3D CNN spatial module plays a crucial role in providing a comprehensive understanding of spatiotemporal dynamics, particularly by considering the spatial distances between adjacent TAZs. The spatial module used in this study compresses the multi-dimensional OD tensor D. The convolution layer takes the input feature vector X and applies convolution operations using the 3D kernel W. Next, the 3D CNN captures the spatial correlations of input data, which is calculated by the following equation. *Max Pooling* (MaxPl) is a downsampling technique commonly used in CNNs to reduce the dimensionality of input data, thereby decreasing the computational effort and minimizing the risk of overfitting. This process involves sliding a kernel W across the input and, at each position, taking the maximum value within the window to form a new, reduced-size output. A detailed description of the 3D CNN model is provided in these papers (Ji et al., 2012; Maturana and Scherer, 2015).

$$X' = \text{Conv3D}(X, W), \tag{2a}$$

$$X'' = \text{MaxPl}(X', W) \tag{2b}$$

where X' represents the output after applying the 3D convolution, and X'' represents the output after applying the 3D max pooling operation

3.1.2. Bi-LSTM layer

The temporal module is designed to capture variations in demand over time. The Bi-LSTM facilitates the effective incorporation of diverse temporal patterns and trends that influence e-scooter demand in future periods. The attention module is strategically introduced to address instances of zero demand in specific zones during certain hours. This lack of activity may be attributed to factors such as nighttime hours or adverse weather conditions. Therefore, the attention module addresses exceptional time periods, such as those influenced by extreme weather, holidays, and weekdays.

The temporal modules in traditional LSTM models focus solely on past information at each time step, potentially limiting their predictive capabilities. To address this limitation, we utilize a Bi-LSTM, which includes an additional backward LSTM layer that processes the input sequence in reverse order within the same time step, as shown in Fig. 4. By combining the hidden states of the forward and backward LSTMs at each time step, the Bi-LSTM captures both past and future dependencies simultaneously. This enables a more comprehensive understanding of the input sequence and improves accuracy in capturing long-term dependencies. Detailed descriptions of the LSTM and Bi-LSTM models are provided in these papers (Sundermeyer et al., 2012; Huang et al., 2015; Yu et al., 2019).

The temporal module used in this study is shown in Fig. 4. The forward pass of the Bi-LSTM can be represented as follows: Forward LSTM unit f_t takes the convolution output vector conv_t and computes the forward hidden state h_t^+ and cell state c_t^+. The backward pass of the Bi-LSTM can be represented as follows: Backward LSTM unit b_t takes the convolution output vector conv_{nt} and computes the backward hidden state h_{nt}^- and cell state c_{nt}^-.

$$h_t^+, c_t^+ = \text{LSTM\_F}(\text{conv}_t, h_{t-1}^+, c_{t-1}^+), \tag{3a}$$

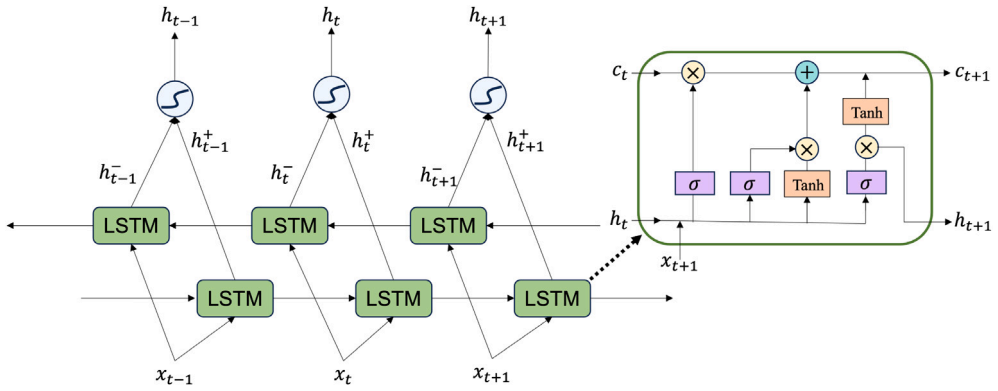

Fig. 4. The Bi-LSTM network.

$$h^-_{nt}, c^-_{nt} = \text{LSTM\_B}(\text{conv}_{nt}, h^-_{nt-1}, c^-_{nt-1}) \tag{3b}$$

The forward and backward hidden state sequences are obtained as follows:

$$H^+ = [h^+_1, h^+_2, \dots, h^+_n], \tag{4a}$$

$$H^- = [h^-_{nt}, h^-_{nt-1}, \dots, h^-_1] \tag{4b}$$

3.1.3. Attention mechanism

The attention mechanism takes the concatenated sequences: forward hidden state H^+, backward hidden state H^-, and the factor vectors Y, and computes the attention scores, followed by generating the context vector. The attention mechanism is thoroughly described in these papers (Chorowski et al., 2015; Liu and Guo, 2019; Niu et al., 2021).

$$\mathrm{s}_t = \mathcal{L}(\text{conc}[H^+, H^-, Y]), \tag{5a}$$

$$\alpha_t = \text{Softmax}(\mathrm{s}_t), \tag{5b}$$

$$z_v = \sum_{t=1}^{N} \alpha_t \cdot x_t, \tag{5c}$$

where x_t represents the elements of the input sequence, and N is the length of the sequence. This equation computes the context vector by summing the element-wise product of the attention weights α_t and the corresponding elements of the input sequence x_t. The loss function (Mean Squared Error, MSE) is adopted to train this model.

$$L(x, \hat{x}) = \frac{1}{F}\|x - \hat{x}\|_2^2 \tag{6}$$

where x is the actual demand data, $\|\cdot\|_2$ is the L2-norm, F is the number of observed data and $\hat{x}$ denotes the predicted demand data.

3.2. Availability assessment

The availability of an e-scooter fleet is evaluated from a comparative perspective by matching current e-scooter locations and energy levels with forthcoming trips. Since the trip predictions are aggregated at the TAZ level, we need to assign them to specific e-scooters to determine whether those trips will be fulfilled. The critical issue is to differentiate between trip ODs and e-scooter usage ODs. There is always some distance to walk before and after using an e-scooter, and this walking distance can be a deciding factor in determining which e-scooter to use or if the traveler will use an e-scooter at all. Therefore, using the starting/ending locations of e-scooter usage (from historical data) as estimations of trip ODs will significantly underestimate the walking distance. When parking zones are enforced, this approach will result in zero walking distance.

To this end, we propose a Monte Carlo-based Trip Assignment Algorithm (MCTA). In MCTA, we first randomly select an origin and destination for each trip in the corresponding OD zones. In the vicinity of the origin point, defined by a predetermined maximum walking distance, we check if there are e-scooters with sufficient battery energy for the trip. If multiple such e-scooters exist, we choose the one with the shortest walking distance and remove it from consideration for other trips. If none exists, we consider the trip unserved. The advantages of the MCTA are twofold. First, it introduces randomness into the locations of origins and destinations, enabling the consideration of walking distance in e-scooter selection. Second, the MCTA is computationally efficient, making it particularly suitable for large-scale fleet analysis. Before presenting the algorithm formally, we provide an example to illustrate the process of availability evaluation.

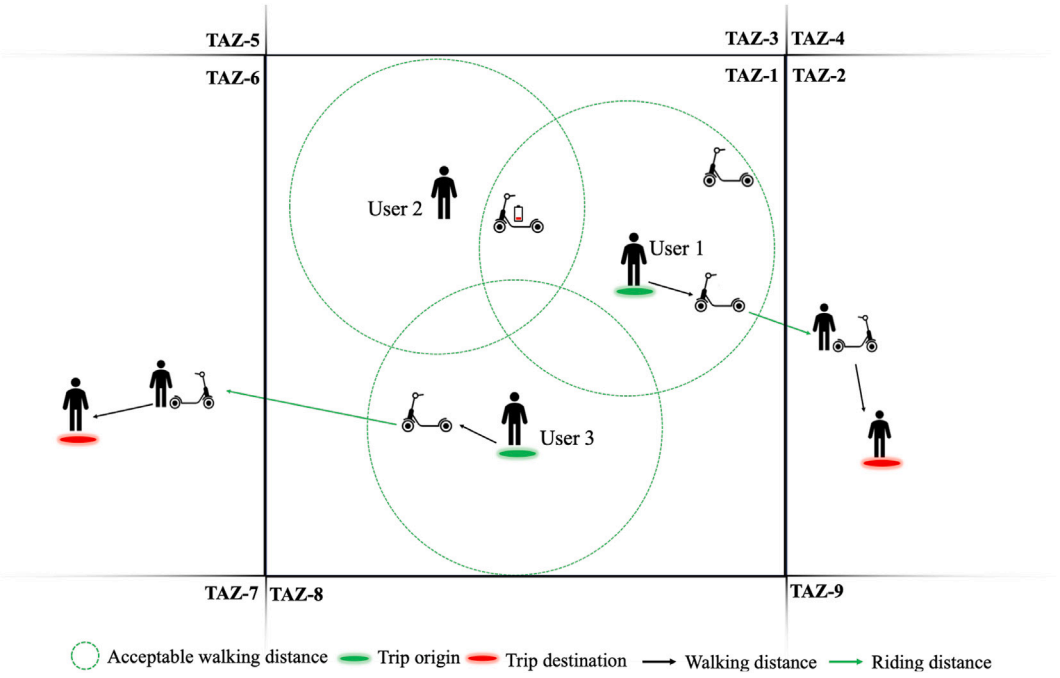

Fig. 5. An example for e-scooter selection.

Consider a scenario with three users positioned at different locations and four e-scooters situated in the same zone (Fig. 5). Each user needs to walk to find an e-scooter to ride. User 1 has three e-scooters within acceptable walking distance, and two of them can sustain the desired trip, so the closest one is picked. User 2 found an e-scooter nearby, but it is depleted and others are too far to walk, so this trip is not fulfilled. User 3 has only one e-scooter nearby, and it is suitable for the trip. Note that we apply a sequential decision-making procedure to avoid two users selecting the same e-scooter, and the priority queue is randomly generated.

The MCTA is formally described in Algorithm 1. Specifically, we introduce two innovative metrics, namely Walking Distance (WD) and Adequate Battery Percent (ABP), to facilitate the calculations. WD represents the minimum distance to the nearest vehicle that has adequate battery energy for the upcoming trip; ABP is the ratio between the number of e-scooters with a sufficient level of SOC and the total number of e-scooters within the maximum walking distance. In the pseudocode, Num is the total iterations for the Monte Carlo Algorithm to achieve a robust availability result. P represents the prediction results for e-scooter OD demand. P_{ram} denotes a random sorting of P to simulate the temporal sequence for users. For every trip k, we randomly generate origins and destinations within their respective origin and destination zones, denoted as $P_{(k,\text{ori})}$, $P_{(k,\text{des})}$. HD is the representation of the Haversine Formula used to calculate the distance between two points. dis_k represents the ride distance for the e-scooter and dis_i represents the walking distance for the user to get an e-scooter. E represents the estimated power consumption elec_k for the upcoming trip k. AW represents the maximum acceptable walking distance for users. SoT represents when the SoC reaches/crosses a certain threshold during a ride, the scooter becomes unavailable to users. av_k represents the available vehicle count for trip k, and nav_k represents the unavailable vehicle count for trip k. A_k record the trip k information about vehicle i, walking distance for the user to get an e-scooter dis_i, and the available vehicle count v_av_k. B_k records the trip k information about the count of unavailable vehicles nav_k. WD_k represents the minimum walking distance in A_k for trip k, and ABP_k represents the sufficient battery percentage for trip k.

In short, this algorithm examines the capability of the e-scooter fleet to fulfill the desired trips sequentially, *i.e.*, one trip after another. The results include not only the ratios of served and unserved trips in each TAZ but also the corresponding walking distances. Moreover, we provide the flow chart in Fig. 6, which should help in better understanding the algorithm's workflow.

4. Case study

In this section, we present a case study using data from the city of Gothenburg, Sweden, to demonstrate the proposed model. We describe the multi-dimensional characteristics of ridership and the tailored hyperparameters for our two-stage model. To demonstrate the effectiveness of the predictive model, we compare it with other prevailing methods, such as GCRN-LSTM. The evaluation results highlight the significance of introducing battery metrics. Finally, we illustrate how constructed environments impact the availability assessment criteria.

Algorithm 1 Monte Carlo-based e-scooter assignment algorithm

for n in Num **do**
  Initial: P_{ram}, av, nav
  for trip k in P_{ram} **do**
    $\text{dis}_k = \text{HD}(P_{(k,\text{ori})}, P_{(k,\text{des})})$
    $\text{elec}_k = \text{E}(\text{dis}_k)$
    for vehicle i in V **do**
      $\text{dis}_i = \text{HD}(P_{(k,\text{ori})}, P_i)$
      if $\text{dis}_i < \text{AW}$ & $\text{elec}_i > \text{elec}_k + \text{SoT}$ **then**
        av_k += 1
        Record $A_k = (i, \text{dis}_i, \text{av}_k)$
      else
        nav_k += 1
        Record $B_k = \text{nav}_k$
      end if
      Record $\text{WD}_k = A_k(\text{Min dis}_i)$
      Record $\text{ABP}_k = \frac{\text{av}_k}{\text{av}_k + \text{nav}_k}$
      Remove WD_k (i) from V
    end for
  end for
  Return average(WD, ABP)
end for

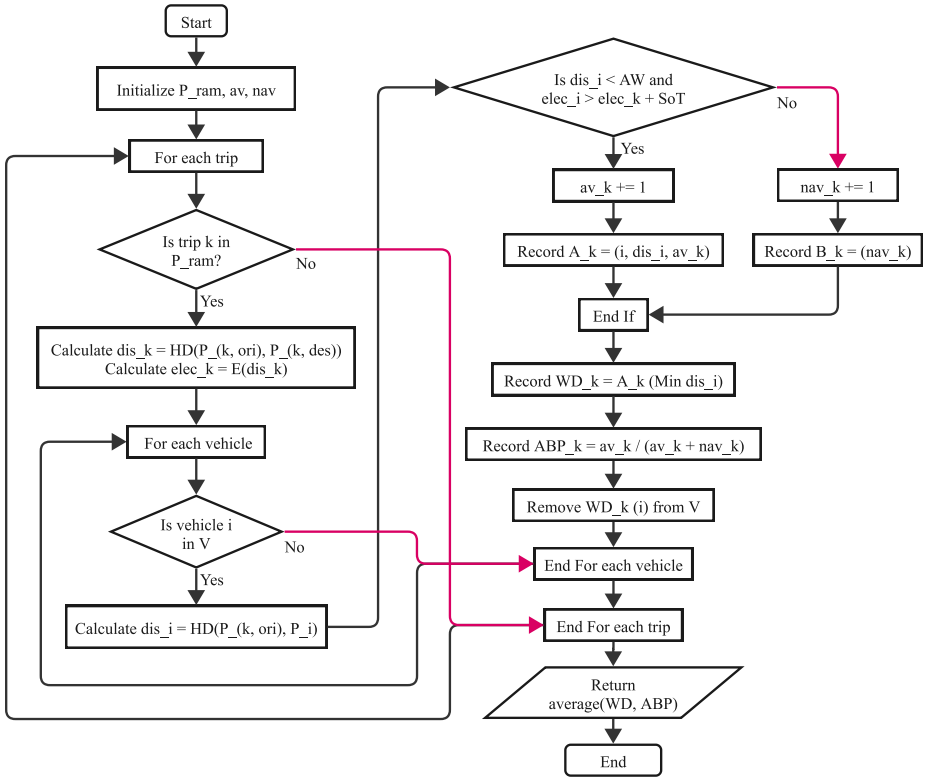

Fig. 6. The flow chart to describe the MCTA .

4.1. Data description

Gothenburg embraced shared e-scooters in 2018 and has since evolved into a mature market. To demonstrate the proposed models, three categories of data were collected over five months from April to September 2023: ridership data from one of the main operators in the city, weather data, and built environment data.

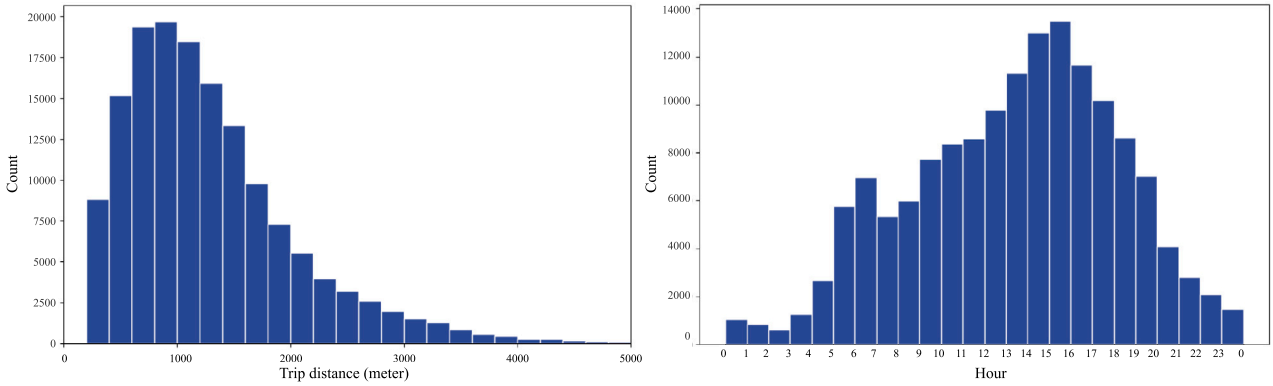

(a) Distribution of trip distance

(b) Average demand variation throughout the day

Fig. 7. Ridership characteristics.

The ridership data is collected through the open API of the operator. The raw data includes positions and battery levels of all usable e-scooters in the city, which excludes those being used. We refresh the data every minute and create an image of the fleet. By cross-checking consecutive images, e-scooter trips can be easily identified. For example, if an e-scooter is missing from an image but rediscovered after 10 min with a reduced battery level, we can reasonably assume that this e-scooter was used for a 10-minute short trip for which energy consumption and trip OD are known. In addition, trips of the following kinds are removed as outliers based on our experience and prior studies in Christoforou et al. (2021) and Merlin et al. (2021). (1) Travel time more than 2 h. This threshold is chosen because e-scooters are typically used for short-distance trips, which are generally completed within a short timeframe, as discussed in Krauss et al. (2024). Additionally, considering the undulating terrain of Gothenburg, we have set the threshold at two hours. (2) Travel distance less than 200 m or longer than 10 km. Very short trips (less than 200 m) may result from GPS drift or minor relocation within a confined area. (3) No energy consumption while traveling more than 2 km. A journey exceeding 2 km without any recorded energy consumption suggests possible data anomalies, such as sensor malfunctions or recording errors. Moreover, when an e-scooter changes its location without consuming energy, it is most likely due to maintenance work, such as repair and relocation.

Our focus is on short-distance trips, which represent the majority of e-scooter usage cases. Excessively long trips might be a combination of multiple trips with short layover times. For example, if the time between the end of one trip and the start of another trip is less than one minute for the same e-scooter, our trip identification methods will fail to separate the two trips. In real-time applications, we exclude such rare cases, given the significant challenges in accurately estimating OD and energy consumption.

In total, 150,915 trips are identified with corresponding travel distances and battery energy consumption. For travel distance estimation, we use Euclidean distance instead of road network distance, a simplification validated by urban transport research findings in Boyacı et al. (2021). In real-world applications, several commercial solutions are available for accurate estimations of trip distance, such as Google Map APIs. The travel distance distribution is shown in Fig. 7(a). We find that for 99.63% of valid trips, the travel distance is within 4000 m. The demand distribution of e-scooters, depicted in Fig. 7(b), is similar to other transportation modes, showing noticeable variations over time. Peaks are observed during the morning rush at 6:00-7:00 and the evening rush at 15:00-16:00.

Similar to the study by Ham et al. (2021), we define a spatial grid size of 500 m per side. Accordingly, the service zone for e-scooters is divided into 578 TAZs, as illustrated in Fig. 8. The spatial trip OD distribution is shown in Fig. 9. The spatial distributions of origins and destinations are slightly different. This similarity can be attributed to two main factors. Firstly, geographical features play a role, as evidenced by a blank area in the southwest due to the Göta River, which separates the area into two activity centers: one in the northwest and the other in the southeast. Secondly, e-scooter usage patterns, primarily serving commuting needs as a last-mile transportation option, lead to close proximity between trip origins and destinations. However, in the city center, where e-scooter usage is frequent, there are notable differences. Zones such as 224, 303, 304, 323, and 324 are hotspots for trip origins, while zones 304, 306, 324, and 364 are hotspots for trip destinations.

Additionally, we examine the relationship between e-scooters' trip distance and battery energy consumption, as shown in Fig. 10. As expected, energy consumption increases with the travel distance increases, albeit with a large variance. The variance in energy consumption may arise from three sources. Firstly, energy consumption is measured by the decrease in SoC, which is a relative metric, and its conversion to absolute energy metrics (such as Wh) hinges on both battery health and the current battery level. A fully charged fresh battery contains much more energy compared to a years-old battery that is nearly depleted if 10% SoC is consumed for both. The second source relates to the terrain of the city. Specifically, a climbing trip consumes more energy than a flat trip with the same travel distance. Gothenburg is a hilly city, which leads to this variance. Lastly, the empirical relationship between energy consumption and travel distance can be disturbed by special use cases, such as when riders take a round trip. In this case, the Euclidean distance between origins and destinations considerably underestimates the real travel distance. Fortunately, such ride patterns account for only 0.87% of all trips, and we exclude them from the data. Therefore, after removing the outliers,

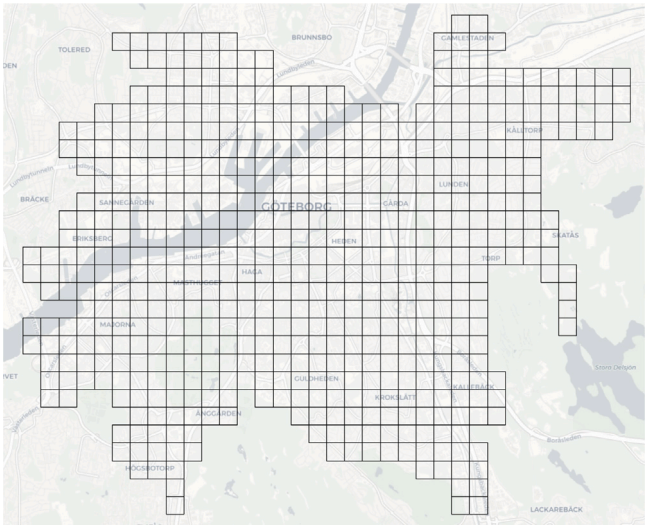

Fig. 8. The TAZ boundaries of the city of Gothenburg.

Table 2
Weather statistical analysis for e-scooter trips in each zone.

Conditions	Min	Max	Mean	Median	Standard deviation	Percent of conditions
Clear	1	1350	76.26	26	150.60	26.62%
Overcast	1	1040	51.83	16	105.78	17.65%
Partially cloudy	1	3341	150.14	43	325.98	53.59%
Rain	1	10	2.14	1	1.73	0.19%
Rain, Overcast	1	30	3.51	2	4.08	0.51%
Rain, Partially cloudy	1	90	6.73	3	10.71	1.42%
Snow, Rain	1	2	1.06	1	0.25	0.02%

Table 3
Simulated trips from predicted OD demand.

Time Interval	Origin		Destination		Distance	Battery consumption
	Zone ID	GPS Coordinates	Zone ID	GPS Coordinates	(meter)	
1	3	(59.3256, 18.0557)	9	(59.3444, 18.0477)	2144.35	6.88%
1	9	(59.3368, 18.0487)	8	(59.3377, 18.0349)	790.49	2.80%
2	5	(59.3338, 18.0728)	4	(59.3300, 18.0603)	827.21	2.80%
2	8	(59.3432, 18.0350)	10	(59.3430, 18.0587)	1347.66	4.51%
3	0	(59.3258, 18.0201)	3	(59.3307, 18.0579)	2218.06	6.88%

we used the mean value to measure the average battery consumption within each distance segment, as shown by the blue line in Fig. 10.

The weather data is obtained from the Visual Crossing Weather website (https://www.visualcrossing.com/) through hourly scraping. Each data record includes temperature, precipitation, wind speed, visibility, and current conditions. The data presented in Table 2 suggest the significant impacts of rain on e-scooter usage. Furthermore, Fig. 11 illustrates a notable trend where e-scooter usage is particularly pronounced when the temperature ranges between 14 to 21 °C. These findings collectively emphasize the significant influence of weather conditions on the choice of e-scooter transportation.

The built environment data is obtained from OpenStreet Map (https://www.openstreetmap.org/node/25930131). The built environment data encompasses six categories: office, dining, transportation, retail, leisure, and residence. The spatial distribution for each category is depicted in Fig. 12. Following this, we compute the intensity of each category within each TAZ.

We transform predicted OD demand into simulated trips, and the workflow as shown in Fig. 13. The yellow part represents actual data, while the green part represents predicted data. For each simulated trip, a random point is generated within the defined origin and destination zone to serve as the trip's simulated origin and simulated destination. Table 3 presents examples of the simulated trips.

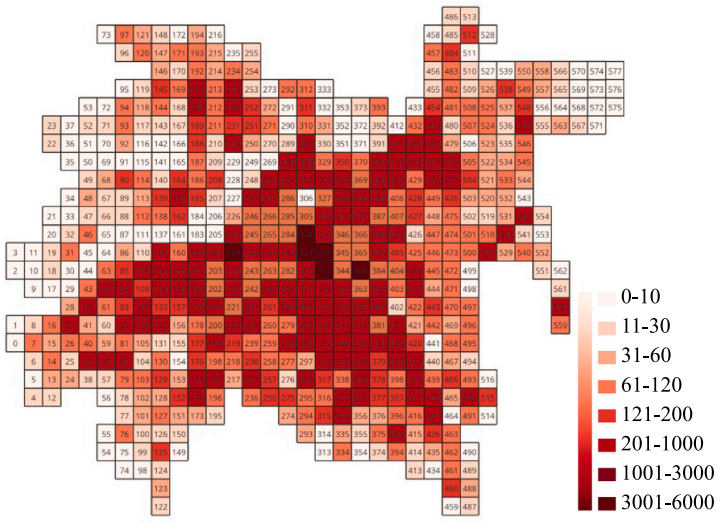

(a) Trip origins distribution

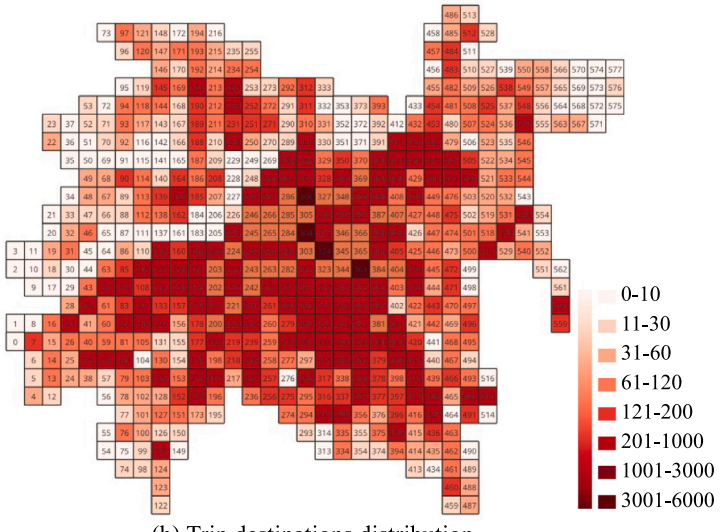

(b) Trip destinations distribution

Fig. 9. The spatial distribution of e-scooter generation within each TAZ.

4.2. Hyperparameters

Hyperparameters are tuned to best resemble the reality in the selected study area. The selected research period totals 168 days. The study's granularity is at the hourly level, and the results are summarized to the average value of all hours. It is noteworthy that, during OD demand prediction, the number of TAZ amounts to 578. This results in a spatial dimension of 578 × 578, consuming a considerable amount of memory space. As described in Fig. 7, e-scooters rarely travel further than 4000 m. Therefore, to alleviate memory usage, we consider only trips that have destinations within a 4000-meter radius around the origin zone. For convenience, we simply it to the 8 surrounding TAZs, since the length of each TAZ equals 500 m. With this approach, we reduce the spatial dimension from 578 × 578 to 578 × 289, representing 578 origin TAZs and 289 destination TAZs. The variable factors are determined by considering weather and time. Weather factors include temperature, precipitation, wind speed, visibility, and overall conditions. Time factors encompass holidays and the day of the week. For categorical features, they are transformed into one-hot encoding. For the input dataset, the number of historical periods L is 6, and the total number of training and test examples K is $168 \times 24 - 6 = 4026$.

For the STAN model, this paper splits the dataset into training and testing sets using a `split_ratio` of 0.8. For the MCTA model, the maximum acceptable walking distance for users is 500 meters (Seneviratne, 1985; Rahul and Verma, 2014). According to empirical observations, e-scooters will not be rentable when their SoCs are below 20%, so the served threshold is 20%.

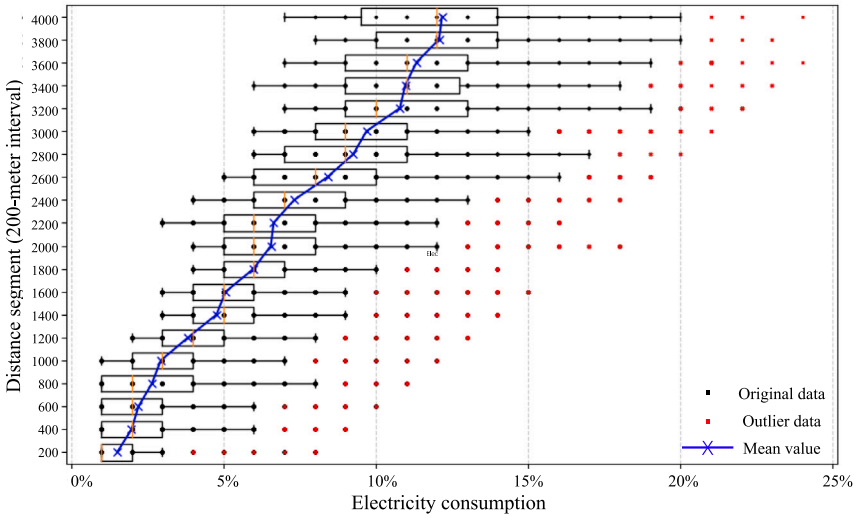

Fig. 10. Box plot of electricity consumption by 200 m distance intervals.

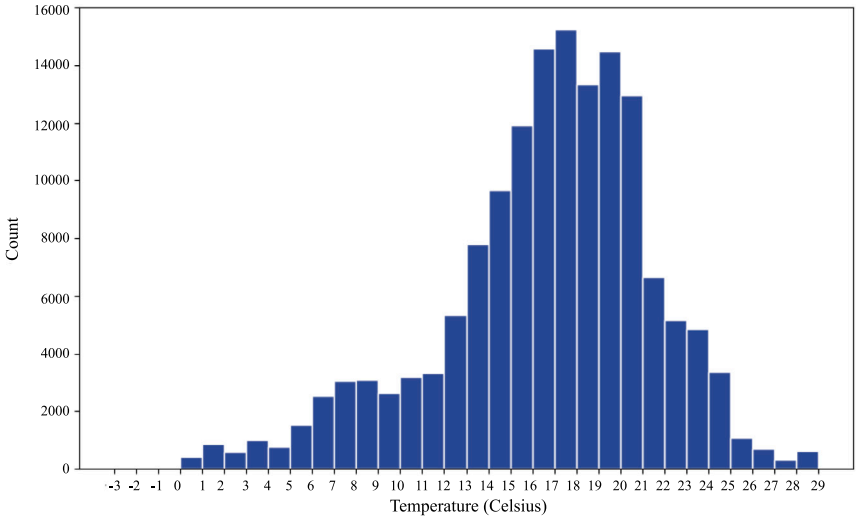

Fig. 11. Temperature conditions for e-scooter trips.

4.3. Prediction results

To conduct a sensitivity analysis for the STAN model, we vary the hyperparameters and observe their impact on model performance. Four metrics are employed to assess the trip prediction results, namely Mean Squared Error (MSE), Root Mean Squared Error (RMSE), Mean Absolute Error (MAE), and Mean Absolute Percentage Error (MAPE). Table 4 presents results across different settings of hidden dimension, learning rate, convolutional kernel size, and epochs. Notably, the hidden state dimension of the bi-LSTM is set to `hidden_dim = 50`, and the learning rate for the Adam optimizer is set to `lr = 0.001`. The size of the convolutional kernel is $3 \times 3 \times 3$. We train the model for `epoch = 400` iterations to optimize its performance. Setting 2 obtains the best performance with an MSE of 0.1156, RMSE of 0.1245, MAE of 0.1532, and MAPE of 14.31%. The RMSE of less than 1 can be attributed to the significant variance in e-scooter usage across different areas. Specifically, while central areas experience high usage frequencies, peripheral regions exhibit much lower usage, sometimes even reaching zero during peak hours. This substantial disparity in usage patterns leads to an overall average that results in an RMSE of less than 1.

To demonstrate predictive effectiveness, we compare the proposed model (STAN) to three benchmark models from existing studies, as well as two variants of STAN. The specifications of the benchmark models are as follows.

- GCRN-LSTM. The Graph Convolutional Recurrent Network (GCRN) model, proposed by Seo et al. (2018), predicts structured and sequential data based on the LSTM model.

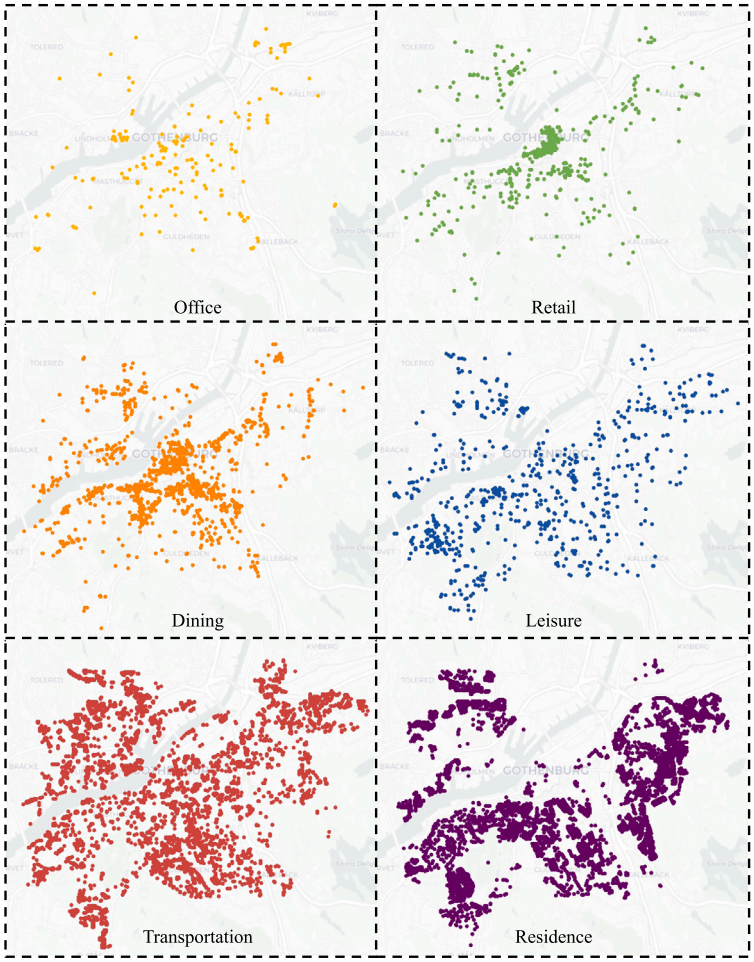

Fig. 12. The spatial distribution of built environment data in the study area.

Table 4
Sensitivity analysis of STAN model hyperparameters.

Setting	Hidden dim	Learning rate	Conv. Kernel size	Epochs	MSE	RMSE	MAE	MAPE (%)
1	25	0.001	3 × 3 × 3	400	0.1183	0.1269	0.1556	14.87
2	50	0.001	3 × 3 × 3	400	**0.1156**	**0.1245**	**0.1532**	**14.31**
3	75	0.001	3 × 3 × 3	400	0.1198	0.1272	0.1563	14.94
4	50	0.0005	3 × 3 × 3	400	0.1205	0.1289	0.1578	15.05
5	50	0.002	3 × 3 × 3	400	0.1213	0.1298	0.1587	15.18
6	50	0.001	2 × 2x2	400	0.1190	0.1267	0.1554	14.79
7	50	0.001	4 × 4x4	400	0.1201	0.1281	0.1566	14.97
8	50	0.001	3 × 3 × 3	300	0.1220	0.1300	0.1593	15.26
9	50	0.001	3 × 3 × 3	500	0.1187	0.1277	0.1560	14.91

- Bi-GRCN. The Bidirectional Graph Recurrent Convolutional Network (Bi-GRCN), proposed by Jiang et al. (2022), predicts taxi flow in Shenzhen.
- GCN-LSTM-Attention. The hybrid prediction method, proposed by Wang et al. (2020b), predicts urban commuters' origin–destination OD.
- CNN-LSTM-Attention. This is the first variant of the proposed model which replaces Bi-LSTM layers with LSTM layers.
- CNN-BiLSTM. This is the second variant of the proposed model which reduces the attention layer.
- STAN-WT. This is the third variant of the proposed model which does not consider weather and time factors.

As demonstrated in Table 5, our model achieved best performance compared to all benchmark models, particularly outperforming GCRN-LSTM by approximately 65.03% in terms of MAE. Additionally, our variation STAN-WT model displays an increase in errors - approximately 33.56% higher MAE and 36.77% higher RMSE compared to our proposed model. When certain factors are omitted,

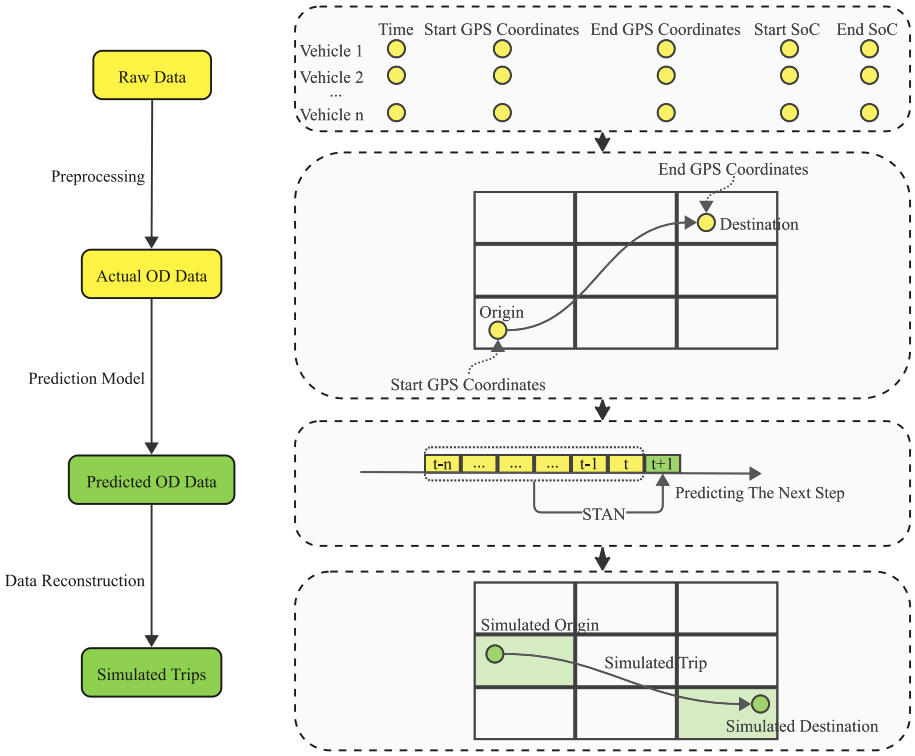

Fig. 13. Workflow from raw data to simulated trips.

Table 5
Prediction results combined different factors.

Model	MSE	MAE	RMSE	MAPE
GCRN-LSTM	0.2453	0.3567	0.3256	25.64%
Bi-GRCN	0.2842	0.3148	0.2987	27.45%
GCN-LSTM-Attention	0.2043	0.2135	0.1934	23.52%
CNN-LSTM-Attention	0.1534	0.1425	0.1745	18.46%
CNN-BiLSTM	0.1683	0.1535	0.1753	16.35%
STAN-WT	0.1864	0.1874	0.2423	20.43%
STAN*	**0.1156**	**0.1245**	**0.1532**	**14.31%**

as in the case of the STAN model without considering these elements, errors notably increase, showing the significance of including specific factors for better predictive accuracy.

4.4. Fleet availability

Based on the predictions, we evaluate the fleet availability of e-scooters using the proposed algorithm in Section 3.2 by examining how many trips are served or unserved. We provide an example to show how to calculate the Availability index for one trip in Fig. 14. "Availability Binary Indicator" is the binary indicator used as the outcome variable in our model. This indicator allows us to predict the availability of e-scooters based on their SoC and walking distance. Since our trip OD prediction model forecasts the demand for the next hour, the spatial distribution and SoC of e-scooters are based on the previous time step's observed data, ensuring that the SoC used for predicting availability reflects the most current observed state.

Additionally, discussing the parameters such as the number of iterations helps to provide a comprehensive view of the algorithm's performance in Table 6. Finally, this paper conducts `times = 100` iterations of Monte Carlo simulations, which resulted in an average battery percentage (ABP) of 93.29% and an average waiting distance (WD) of 119.52 m.

Regarding the details of the comparison, we provide the formula used to calculate availability in the two groups (static threshold group and our method), respectively, to communicate more precisely and conveniently. For the static threshold group,

$$A^{s}_{i,t+1} = \frac{n_{i,t}(SoC < 20\%)}{N_{i,t}} \tag{7}$$

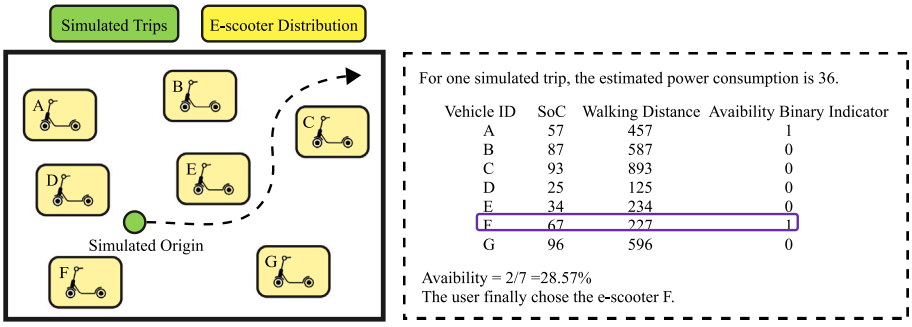

Fig. 14. An example of calculating the Availability index for one trip.

Table 6
Results of different iterations for the MCTA algorithm.

Setting	Number of iterations	ABP (%)	WD (meters)
1	50	93.12	128.45
2	80	92.57	110.32
3	**100**	**93.29**	**119.52**
4	120	94.05	121.67

where $A^{s}_{i,t+1}$ denotes the availability for zone i at time $t+1$; $n_{i,t}(SoC < 20\%)$ denotes the number of e-scooters having SoC lower than 20% at time t; $N_{i,t}$ denotes the total number of vehicles in zone i at time t. It is irrelevant to future demand, so we use the current fleet status at time t to infer future availability at time $t+1$, and this is currently being used in the industry. Therefore, in both groups, we use observed SoC values in the current time step to predict availability in the next time step. The spatial distribution of average e-scooter unavailability is plotted, as shown in Fig. 15. Our model indicates that 6.71% of the fleet is unavailable on average, while the benchmark group in Fig. 15(b) reports an average ratio of 3.87%. Considering the large fleet sizes currently operating in cities that can amount to several thousands of e-scooters, this underestimation is nontrivial. More importantly, the distribution of underserved zones is dissimilar, which will lead to totally different operational practices. For example, zone 142 has a few e-scooters with low battery levels, but it should not be on top of the charging list, since there is almost no demand either. In contrast, zone 70 has e-scooters with healthy (SoC> 20%) battery levels that are insufficient to fulfill forthcoming trips.

The average number of e-scooters available at various times throughout the day is summarized in Fig. 16. The peak numbers occur at 8 a.m. and 3 p.m., aligning with the peak commuting times in Gothenburg. This link may appear counterintuitive since those are hours with higher demand. We believe the rise in availability measures is primarily attributed to the operator's charging operations, which are also performed during those hours based on our field data. Specifically, around 240 e-scooters were charged through battery swapping in three-time slots: 6 a.m. to 9 a.m., 3 p.m. to 6 p.m., and 11 p.m. to 1 a.m. Fig. 17 shows the spatial distribution of average e-scooter availability at 7 a.m. and 8 a.m., respectively. The color gradient indicates the percentage of available scooters, with darker shades representing higher availability. These peak commuting hours see increased availability due to the targeted charging operations by the operators. This suggests that the proposed model is resilient to demand variations and can accurately reflect operational activities.

Moreover, we present the walking distance distributions in Fig. 18. The average walking distance to get a usable e-scooter is 119.52 m. In city centers, the walking distance is generally less than 90 m due to the high density of e-scooters. As the city expands outward from its center, the walking distance for users gradually increases, indicating a decline in the service level of e-scooters in the peripheral areas of the city.

4.5. Partial dependence plot for availability

The Partial Dependence Plot (PDP) is a commonly used tool in machine learning to examine the relationship between specific features and the target prediction while holding other features constant. PDP is advantageous because it can show how changes in specific features affect the target variable, offering insights into the model's performance. The PDP technique allows us to examine how built environments impact availability assessment criteria, specifically walking distance (WD) and adequate battery percent (ABP).

The PDP outcomes for the built environment and walking distance are shown in Fig. 19. The y-axis represents walking distance, while the x-axis represents the number of different POIs. Thus, the figure illustrates how changes in each category of POI affect walking distance. A noticeable negative association is observed between the proximity of food-related establishments and the availability index when analyzing walking distance data. Shorter access times to e-scooters are linked to proximity to amenities in the area. Conversely, regions around transportation hubs and residential areas experience significant changes in availability, suggesting that consumers might have to travel a distance to reach vehicles. For instance, starting a ride after leaving a bus station platform or moving through residential areas would require covering a significant distance to get to the closest e-scooter. The

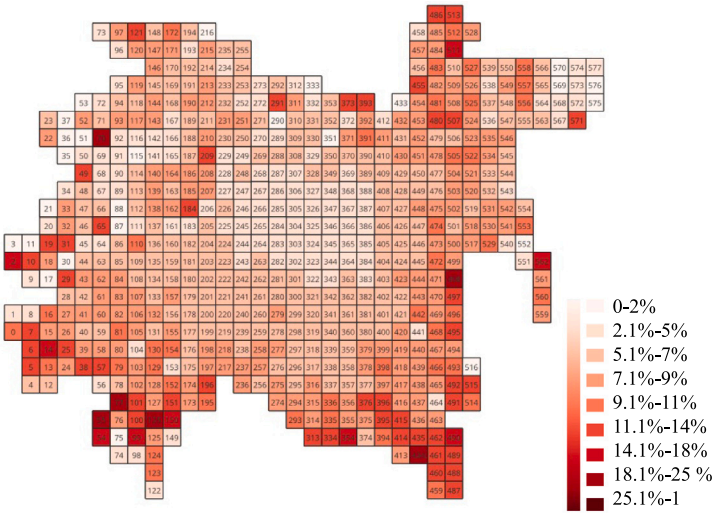

(a) The spatial distribution of average e-scooter unavailability based on the proposed method

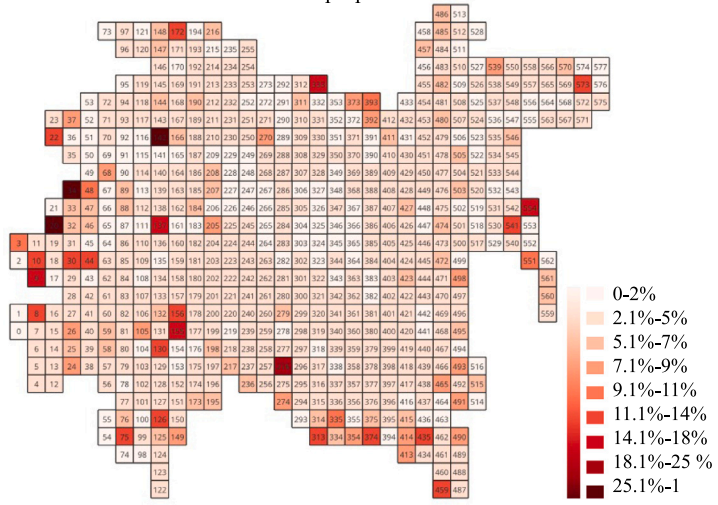

(b) The spatial distribution of average e-scooter unavailability based on criterion SoC<20%

Fig. 15. The spatial distribution of average e-scooter unavailability with different metrics.

variation in access times across different locations highlights the subtle influence of the built environment on e-scooter availability. These studies highlight the intricate nature of accessibility patterns affected by the built environment, essential aspects to consider when optimizing the placement and distribution methods for e-scooter deployment in urban areas (Schwanen and Mokhtarian, 2005; Zhou, 2022).

The PDP results for the built environment and walking distance are depicted in Fig. 20. Similarly, the *y*-axis represents the percentage of availability, and the *x*-axis represents the number of various POIs. Therefore, the figure reflects the impact of changes in each type of POI on e-scooter availability. The observed correlation between the percent of available e-scooters and dining-related labels reveals a discernible positive relationship, indicating a proportional rise in e-scooter availability around dining establishments. Conversely, residential and transportation labels depict more erratic trends in availability metrics. Within transportation labels, the substantial variability can be attributed to diverse user travel patterns, leading to fluctuations in e-scooter accessibility. Notably, leisure-related labels register a count of zero within the value range of ten, indicating a complete absence of available vehicles in these areas. This finding suggests potential restrictions on e-scooter deployment in expansive parks or green spaces, resulting in a dearth of available vehicles within their proximity. Our analysis aligns with observations from the Tier app, which shows that parking is prohibited in these areas. This exploration indicates the different impacts of various location types on e-scooter availability. The positive correlation with dining-related establishments underscores the higher concentration of available vehicles in dining areas, possibly influenced by increased user demand or optimized deployment strategies. Conversely, the absence of available e-scooters

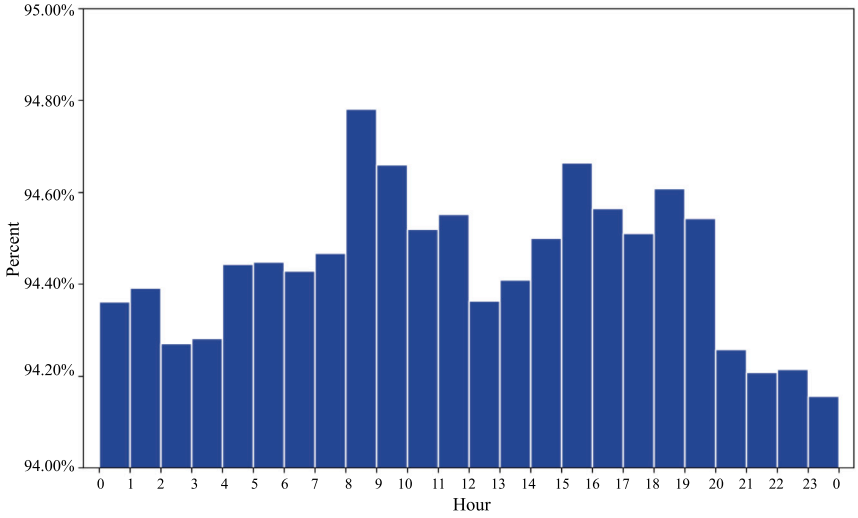

Fig. 16. The percent of average e-scooter availability in each hour.

in leisure-related zones suggests regulatory or logistical limitations in these expansive areas, warranting further investigation into potential restrictions impacting e-scooter accessibility.

5. Conclusion and discussion

This paper proposes a two-stage e-scooter availability prediction model for shared e-scooters. In the first stage, the STAN model is developed to predict the origin–destination demand for e-scooter trips. In the second stage, the MCTA model is employed to examine the ratios of trips that are effectively served by considering walking distance and battery levels. The novelty of this research lies in the incorporation of battery metrics, resulting in more realistic predictions of e-scooter availability. The results of the STAN model show an MSE of 0.1156, RMSE of 0.1245, MAE of 0.1532, and MAPE of 14.31%, demonstrating the model's effectiveness. In comparison to the current practice that considers only SoC levels below 20%, the proposed method reports not only a 73.3% higher percentage of unserved trips but also a distinct spatial distribution. The average walking distance for users to ride an e-scooter is observed to be approximately 120 m. The PDP analysis reveals a multifaceted relationship between users' walking distance, the percentage of available e-scooters, and different location labels. Notably, dining-related labels demonstrate obvious negative correlations with walking distance and positive correlations with vehicle availability.

The direct beneficiaries are e-scooter operators. In practice, fleet availability can change considerably within a short period. Since maintenance operations such as battery swapping and relocation can take some time, observation-based operations may be misleading. Prediction-based operations, however, can more effectively address real needs and enhance responsiveness to demand variations. Furthermore, our research has important implications for policy-making in urban mobility and e-scooter regulation. In comparison to the static threshold, our method may produce significantly different results regarding fleet availability and is more reliable due to the consideration of demand factors (*e.g.*, the desired battery SoC). The new results can better inform municipalities about the service quality of e-scooter operators, which may lead to changes in the standards used in permit issuing, monitoring, and regulations.

Despite the promising potential of our predictive model for enhancing e-scooter service efficiency and user satisfaction, several limitations must be addressed. The model's reliance on extensive real-time data collection and processing presents a significant challenge for practical implementation, necessitating substantial computational resources. Simplifying the model or using it selectively during peak periods could mitigate this issue. Additionally, the complexity of our approach might pose challenges for policymakers who typically rely on straightforward observational data; hence, observed availability may often suffice for regulatory purposes. Another limitation is the uniform shape and area of the TAZs in our model, which do not accurately reflect typical urban landscapes. Future work should incorporate more realistic TAZ divisions to improve model precision. Finally, Euclidean distance does not account for real-world factors such as traffic patterns, road infrastructure, and barriers like rivers or highways, which can influence actual travel times and paths taken by e-scooter users. This simplification may lead to inaccuracies in estimating travel distances and consequently affect predictions related to e-scooter availability and usage patterns. An effective solution could involve utilizing the Google Maps API, which calculates distances closer to reality by considering factors such as traffic patterns, road infrastructure, and obstacles. By addressing these limitations and advancing our model, we aim to contribute to more robust and sustainable urban mobility solutions that effectively leverage the potential of e-scooters. Our work paves the way for future studies in this field.

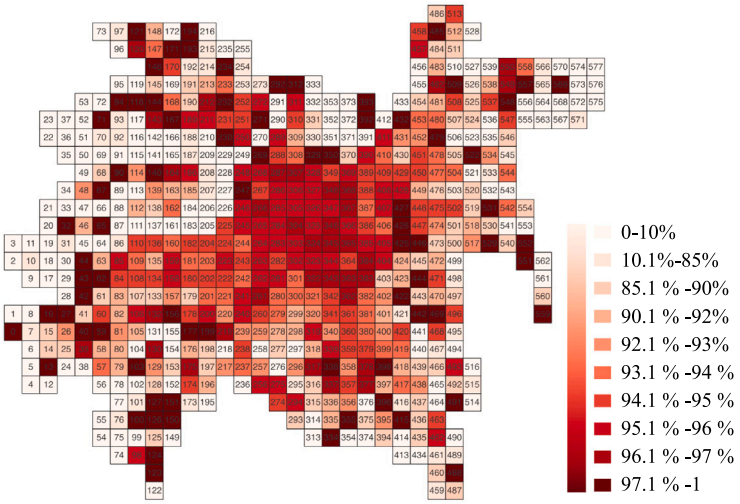

(a) The spatial distribution of average e-scooter availability at 7 AM

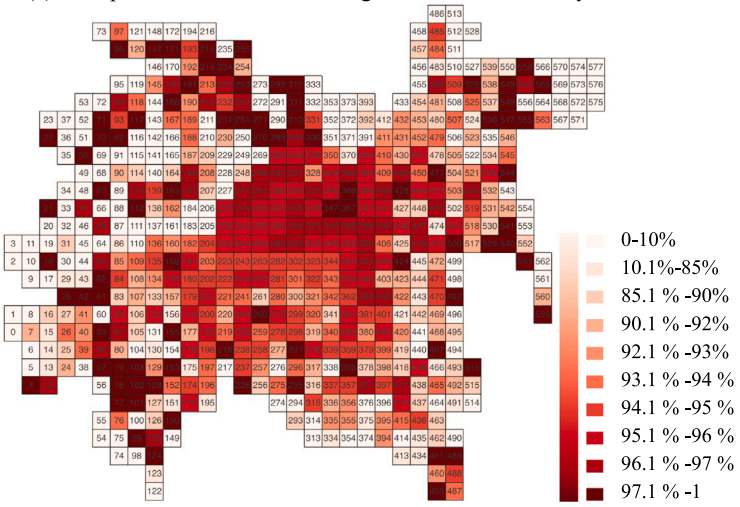

(b) The spatial distribution of average e-scooter availability at 8 AM

Fig. 17. The spatial distribution of average e-scooter availability.

CRediT authorship contribution statement

Jiahui Zhao: Writing – original draft, Visualization, Methodology, Formal analysis, Data curation, Conceptualization. **Jiaming Wu:** Writing – review & editing, Visualization, Supervision, Methodology, Funding acquisition, Formal analysis, Conceptualization. **Zhibin Li:** Writing – review & editing, Supervision. **Pan Liu:** Writing – review & editing, Supervision, Funding acquisition.

Data availability

Data and code are shared via Github (see appendix in the paper)

Acknowledgments

This work was supported by the Swedish Energy Agency, Sweden under project FEAT (P2022-00404), and Energy Area of Advance at Chalmers University of Technology, Sweden under project "Energy efficiency analysis for co-existing shared and electric micromobility". This work was also supported by the Postgraduate Research & Practice Innovation Program of Jiangsu Province, China under grant number KYCX22_0274.

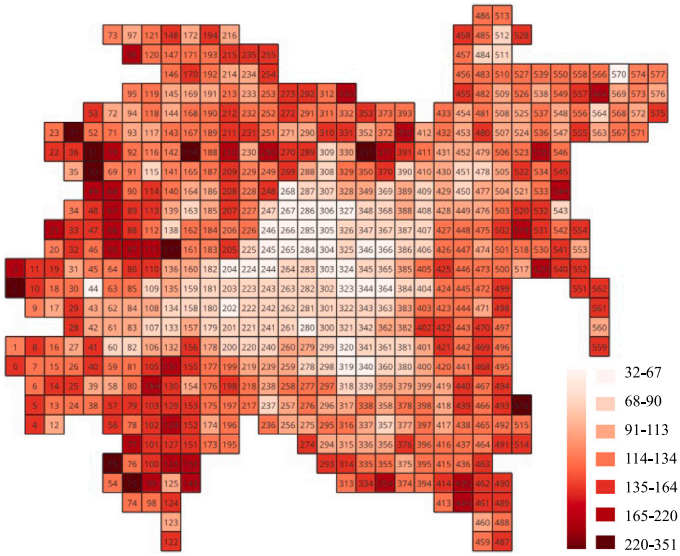

Fig. 18. The spatial distribution for users' walking distance.

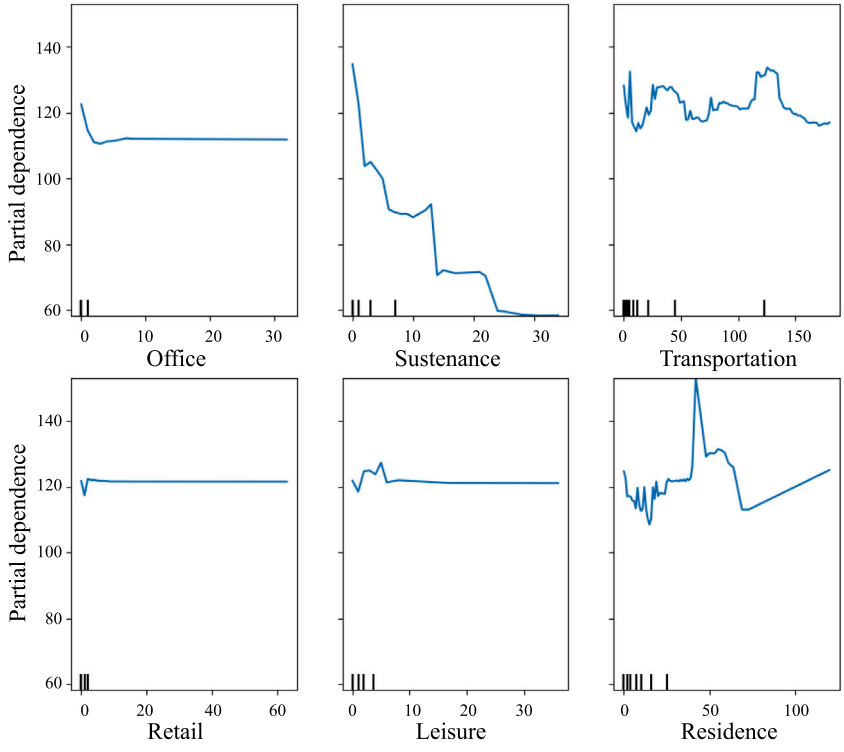

Fig. 19. The PDP analysis for the assessment metrics of availability: walking distance.

Appendix

The sample data and code are available for download through the following GitHub link, https://github.com/jhZzz021/The-program-for-our-work.git.

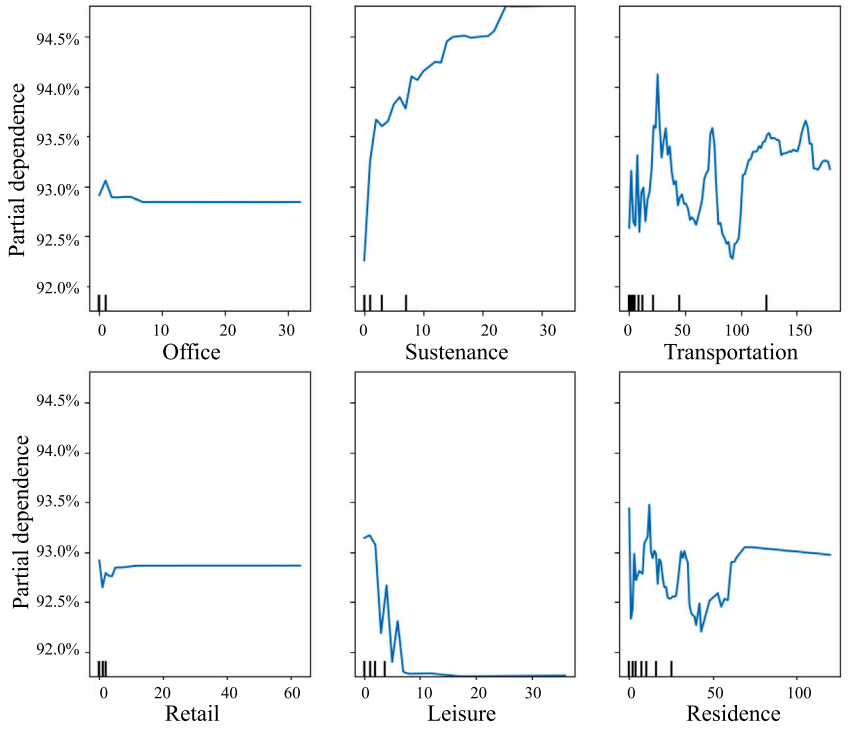

Fig. 20. The PDP analysis for the assessment metrics of availability: available percent for e-scooters.

Table 7
Abbreviations.

Term	Abbreviation
Adequate Battery Percent	ABP
Three-dimensional Convolutional Neural Network	3D CNN
Bidirectional Long Short-Term Memory Neural Network	Bi-LSTM
SpatioTemporalAttentionNet model	STAN
State of Charge	SoC
Traffic Analysis Zones	TAZs
Walking Distance	WD
Origins and Destinations	OD

Abbreviation list

For a comprehensive overview of the terminology and abbreviations utilized throughout our paper, refer to Table 7.

References

6T Research Office, 2019. Uses and users of free-floating electric scooters in France. URL https://shorturl.at/ahrO2.

Afandizadeh Zargari, S., Memarnejad, A., Mirzahossein, H., 2021. Hourly origin–destination matrix estimation using intelligent transportation systems data and deep learning. Sensors 21 (21), 7080.

Almannaa, M.H., Elhenawy, M., Rakha, H.A., 2020. Dynamic linear models to predict bike availability in a bike sharing system. Int. J. Sustain. Transp. 14 (3), 232–242.

Altintasi, O., Yalcinkaya, S., 2022. Siting charging stations and identifying safe and convenient routes for environmentally sustainable e-scooter systems. Sustainable Cities Soc. 84, 104020.

Anderson, I., 2022. Electric scooter revolution faces a reckoning in stockholm. URL https://www.bloomberg.com/news/articles/2022-08-20/stockholm-targets-electric-scooters-with-more-restrictions?embedded-checkout=true.

Ashqar, H.I., Elhenawy, M., Almannaa, M.H., Ghanem, A., Rakha, H.A., House, L., 2017. Modeling bike availability in a bike-sharing system using machine learning. In: 2017 5th IEEE International Conference on Models and Technologies for Intelligent Transportation Systems (MT-ITS). IEEE, pp. 374–378.

Askari, S., Javadinasr, M., Peiravian, F., Khan, N.A., Auld, J., Mohammadian, A.K., 2024. Loyalty toward shared e-scooter: Exploring the role of service quality, satisfaction, and environmental consciousness. Travel Behav. Soc. 37, 100856.

Ayyildiz, E., 2022. A novel pythagorean fuzzy multi-criteria decision-making methodology for e-scooter charging station location-selection. Transp. Res. D 111, 103459.

Bai, S., Jiao, J., 2021. Toward equitable micromobility: Lessons from austin e-scooter sharing program. J. Plann. Educ. Res. 0739456X211057196.
Boyacı, B., Dang, T.H., Letchford, A.N., 2021. Vehicle routing on road networks: How good is Euclidean approximation? Comput. Oper. Res. 129, 105197.
Buchmann, I., 2003. How to prolong lithium-based batteries. Batter. Portable World 15, 2–3.
Butt, M.A., Danjuma, S., Ilyas, M.S.B., Butt, U.M., Shahid, M., Tariq, I., 2023. Demand prediction on bike sharing data using regression analysis approach. J. Innov. Comput. Emerg. Technol. 3 (1).
Button, K., Frye, H., Reaves, D., 2020. Economic regulation and E-scooter networks in the USA. Res. Transp. Econ. 84, 100973.
Carrese, S., Giacchetti, T., Nigro, M., Algeri, G., Ceccarelli, G., 2021. Analysis and management of e-scooter sharing service in Italy. In: 2021 7th International Conference on Models and Technologies for Intelligent Transportation Systems (MT-ITS). IEEE, pp. 1–7.
Chorowski, J.K., Bahdanau, D., Serdyuk, D., Cho, K., Bengio, Y., 2015. Attention-based models for speech recognition. Adv. Neural Inf. Process. Syst. 28.
Christoforou, Z., de Bortoli, A., Gioldasis, C., Seidowsky, R., 2021. Who is using e-scooters and how? Evidence from Paris. Transp. Res. D 92, 102708.
Department for Transport, 2022. National evaluation of e-scooter trials. URL https://shorturl.at/aivHI.
Ding, C., Cao, X., Dong, M., Zhang, Y., Yang, J., 2019. Non-linear relationships between built environment characteristics and electric-bike ownership in Zhongshan, China. Transp. Res. D 75, 286–296.
Drimlová, E., Šucha, M., Rečka, K., Haworth, N., Fyhri, A., Wallgren, P., Silverans, P., Slootmans, F., et al., 2024. Attitudes towards E-scooter safety-A survey in five countries. Trans. Transp. Sci.
Engdahl, H., Englund, C., Faxér, A., Habibi, S., Pettersson, S., Sprei, F., Voronov, A., Wedlin, J., 2020. Electric scooters' trip data collection and analysis. In: Proceedings of the 33rd Electric Vehicle Symposium (EVS33), Portland, Oregon. pp. 14–17.
Fearnley, N., 2020. Micromobility–regulatory challenges and opportunities. In: Shaping Smart Mobility Futures: Governance and Policy Instruments in Times of Sustainability Transitions. Emerald Publishing Limited, pp. 169–186.
Feng, C., Jiao, J., Wang, H., 2022. Estimating e-scooter traffic flow using big data to support planning for micromobility. J. Urban Technol. 29 (2), 139–157.
Fietz, L.E., 2020. Predicting Hourly Shared E-Scooter Use in Chicago: A Machine Learning Approach (Ph.D. thesis). University of Oregon.
Foissaud, N., Gioldasis, C., Tamura, S., Christoforou, Z., Farhi, N., 2022. Free-floating e-scooter usage in urban areas: A spatiotemporal analysis. J. Trans. Geogr. 100, 103335.
Ge, Y.-E., Long, J., Xiao, F., Shi, Q., 2018. Traffic modeling for low-emission transport. Transp. Res. D 60, 1–6.
Giordano, M., Chow, J.Y., 2024. An e-scooter service region and fleet allocation design problem with elastic demand. Transp. Res. D 130, 104153.
Guidon, S., Reck, D.J., Axhausen, K., 2020. Expanding a (n)(electric) bicycle-sharing system to a new city: Prediction of demand with spatial regression and random forests. J. Transp. Geogr. 84, 102692.
Guo, Z., Liu, J., Zhao, P., Li, A., Liu, X., 2023. Spatiotemporal heterogeneity of the shared e-scooter–public transport relationships in Stockholm and Helsinki. Transp. Res. D 122, 103880.
Ham, S.W., Cho, J.-H., Park, S., Kim, D.-K., 2021. Spatiotemporal demand prediction model for e-scooter sharing services with latent feature and deep learning. Transp. Res. Record 2675 (11), 34–43.
He, S., Shin, K.G., 2020. Dynamic flow distribution prediction for urban dockless e-scooter sharing reconfiguration. In: Proceedings of the Web Conference 2020. pp. 133–143.
Hollingsworth, J., Copeland, B., Johnson, J.X., 2019. Are e-scooters polluters? The environmental impacts of shared dockless electric scooters. Environ. Res. Lett. 14 (8), 084031.
Hosseinzadeh, A., Karimpour, A., Kluger, R., 2021. Factors influencing shared micromobility services: An analysis of e-scooters and bikeshare. Transp. Res. D 100, 103047.
Huang, Z., Xu, W., Yu, K., 2015. Bidirectional LSTM-CRF models for sequence tagging. arXiv preprint arXiv:1508.01991.
Iolov, T.V., 2022. Milan to curb e-scooters and operators next year. URL https://shorturl.at/nwAL8.
Jain, A., Jha, V., Alsaif, F., Ashok, B., Vairavasundaram, I., Kavitha, C., 2024. Machine learning framework using on-road realtime data for battery soc level prediction in electric two-wheelers. J. Energy Storage 97, 112884.
Ji, S., Cherry, C.R., Han, L.D., Jordan, D.A., 2014. Electric bike sharing: simulation of user demand and system availability. J. Clean. Prod. 85, 250–257.
Ji, S., Xu, W., Yang, M., Yu, K., 2012. 3D convolutional neural networks for human action recognition. IEEE Trans. Pattern Anal. Mach. Intell. 35 (1), 221–231.
Jiang, W., Xiao, Y., Liu, Y., Liu, Q., Li, Z., et al., 2022. Bi-GRCN: A spatio-temporal traffic flow prediction model based on graph neural network. J. Adv. Transp. 2022.
Jiao, J., Bai, S., 2020. Understanding the shared e-scooter travels in Austin, TX. ISPRS Int. J. Geo-Inf. 9 (2), 135.
Jin, S.T., Sui, D.Z., 2024. A comparative analysis of the spatial determinants of e-bike and e-scooter sharing link flows. J. Transp. Geogr. 119, 103959.
Kabra, A., Belavina, E., Girotra, K., 2020. Bike-share systems: Accessibility and availability. Manage. Sci. 66 (9), 3803–3824.
Karimpour, A., Hosseinzadeh, A., Kluger, R., 2023. A data-driven approach to estimating dockless electric scooter service areas. J. Transp. Geogr. 109, 103579.
Kazemzadeh, K., Sprei, F., 2022. Towards an electric scooter level of service: A review and framework. Travel Behav. Soc. 29, 149–164.
Kim, S., Choo, S., Lee, G., Kim, S., 2022. Predicting demand for shared e-scooter using community structure and deep learning method. Sustainability 14 (5), 2564.
Krauss, K., Gnann, T., Burgert, T., Axhausen, K.W., 2024. Faster, greener, scooter? An assessment of shared e-scooter usage based on real-world driving data. Transp. Res. A 181, 103997.
Lee, M., Chow, J.Y., Yoon, G., He, B.Y., 2021. Forecasting e-scooter substitution of direct and access trips by mode and distance. Transp. Res. D 96, 102892.
Leurent, F., 2022. What is the value of swappable batteries for a shared e-scooter service? Res. Transp. Bus. Manag. 45, 100843.
Li, A., Zhao, P., Liu, X., Mansourian, A., Axhausen, K.W., Qu, X., 2022. Comprehensive comparison of e-scooter sharing mobility: Evidence from 30 European cities. Transp. Res. D 105, 103229.
Liu, G., Guo, J., 2019. Bidirectional LSTM with attention mechanism and convolutional layer for text classification. Neurocomputing 337, 325–338.
Liu, S., Hou, J., Liu, Y., Khadka, A., Liu, Z., 2018. OD demand forecasting for the large-scale dockless sharing bike system: a deep learning approach. In: 18th COTA International Conference of Transportation Professionals. American Society of Civil Engineers Reston, VA, pp. 1683–1692.
Liu, X., Liu, X.C., Liu, Z., Shi, R., Ma, X., 2023. A solar-powered bus charging infrastructure location problem under charging service degradation. Transp. Res. D 119, 103770.
Liu, M., Seeder, S., Li, H., et al., 2019. Analysis of e-scooter trips and their temporal usage patterns. Inst. Transp. Eng. ITE J. 89 (6), 44–49.
Ma, Q., Yang, H., Mayhue, A., Sun, Y., Huang, Z., Ma, Y., 2021. E-scooter safety: The riding risk analysis based on mobile sensing data. Accid. Anal. Prev. 151, 105954.
Makkawi Gassim, H.A., 2024. Micro-Mobility Vehicles: Current Regulatory Framework and Possible Solutions to Improve Safety for the Road User (Ph.D. thesis). Politecnico di Torino.
Maturana, D., Scherer, S., 2015. Voxnet: A 3d convolutional neural network for real-time object recognition. In: 2015 IEEE/RSJ International Conference on Intelligent Robots and Systems. IROS, IEEE, pp. 922–928.
May, T., 2023. Micromobility operators publish industry recommendations for E-scooters | future transport-news. URL https://futuretransport-news.com/micromobility-operators-publish-industry-recommendations-for-e-scooters/,
Merlin, L.A., Yan, X., Xu, Y., Zhao, X., 2021. A segment-level model of shared, electric scooter origins and destinations. Transp. Res. D 92, 102709.
Mitropoulos, L., Stavropoulou, E., Tzouras, P., Karolemeas, C., Kepaptsoglou, K., 2023. E-scooter micromobility systems: Review of attributes and impacts. Transp. Res. Interdiscipl. Perspect. 21, 100888.

Nacto Bike Share, 2015. Walkable station spacing is key to successful, equitable bike share. URL https://shorturl.at/epNO8.
Nadkarni, R., 2020. Managing E-scooter-rentals in German cities: A check-up. Deutsches Institut für Urbanistik.
Nikiforiadis, A., Paschalidis, E., Stamatiadis, N., Raptopoulou, A., Kostareli, A., Basbas, S., 2021. Analysis of attitudes and engagement of shared e-scooter users. Transp. Res. D 94, 102790.
Niu, Z., Zhong, G., Yu, H., 2021. A review on the attention mechanism of deep learning. Neurocomputing 452, 48–62.
Orvin, M.M., Bachhal, J.K., Fatmi, M.R., 2022. Modeling the demand for shared e-scooter services. Transp. Res. Record 2676 (3), 429–442.
Osorio, J., Lei, C., Ouyang, Y., 2021. Optimal rebalancing and on-board charging of shared electric scooters. Transp. Res. B 147, 197–219.
Phithakkitnukooon, S., Patanukhom, K., Demissie, M.G., 2021. Predicting spatiotemporal demand of dockless e-scooter sharing services with a masked fully convolutional network. ISPRS Int. J. Geo-Inf. 10 (11), 773.
Rahul, T., Verma, A., 2014. A study of acceptable trip distances using walking and cycling in bangalore. J. Transp. Geogr. 38, 106–113.
Rechkemmer, S.K., Zhang, W., Sawodny, O., 2017. Modeling of a permanent magnet synchronous motor of an e-scooter for simulation with battery aging model. IFAC-PapersOnLine 50 (1), 4769–4774.
Reck, D.J., Martin, H., Axhausen, K.W., 2022. Mode choice, substitution patterns and environmental impacts of shared and personal micro-mobility. Transp. Res. D 102, 103134.
Roberts, G., 2023. E-scooters banned in Paris; poll suggests UK motorists also want ban. URL https://shorturl.at/dgTV9.
Sareen, S., Remme, D., Haarstad, H., 2021. E-scooter regulation: The micro-politics of market-making for micro-mobility in Bergen. Environ. Innov. Soc. Trans. 40, 461–473.
Sathishkumar, V., Park, J., Cho, Y., 2020. Using data mining techniques for bike sharing demand prediction in metropolitan city. Comput. Commun. 153, 353–366.
Saum, N., Sugiura, S., Piantanakulchai, M., 2020. Short-term demand and volatility prediction of shared micro-mobility: a case study of e-scooter in thammasat university. In: 2020 Forum on Integrated and Sustainable Transportation Systems. FISTS, IEEE, pp. 27–32.
Schwanen, T., Mokhtarian, P.L., 2005. What if you live in the wrong neighborhood? The impact of residential neighborhood type dissonance on distance traveled. Transp. Res. D 10 (2), 127–151.
Seneviratne, P.N., 1985. Acceptable walking distances in central areas. J. Transp. Eng. 111 (4), 365–376.
Seo, Y., Defferrard, M., Vandergheynst, P., Bresson, X., 2018. Structured sequence modeling with graph convolutional recurrent networks. In: Neural Information Processing: 25th International Conference, ICONIP 2018, Siem Reap, Cambodia, December 13-16, 2018, Proceedings, Part I 25. Springer, pp. 362–373.
Sexton, E.G., Harmon, K.J., Sanders, R.L., Shah, N.R., Bryson, M., Brown, C.T., Cherry, C.R., 2023. Shared e-scooter rider safety behaviour and injury outcomes: a review of studies in the United States. Transp. Rev. 1–23.
Song, J.-C., Hsieh, I.-Y.L., Chen, C.-S., 2023. Sparse trip demand prediction for shared E-scooter using spatio-temporal graph neural networks. Transp. Res. D 125, 103962.
Statista, 2023. E-scooter-sharing: market data & analysis. URL https://www.statista.com/outlook/mmo/shared-mobility/e-scooter-sharing/worldwide,
Study in Torino, 2020. Electric scooters arrive in Torino. URL https://shorturl.at/zAFOS.
Sundermeyer, M., Schlüter, R., Ney, H., 2012. Lstm neural networks for language modeling. In: Interspeech. 2012, pp. 194–197.
Tuli, F.M., Mitra, S., Crews, M.B., 2021. Factors influencing the usage of shared E-scooters in chicago. Transp. Res A 154, 164–185.
Wang, K., Qian, X., Fitch, D.T., Lee, Y., Malik, J., Circella, G., 2023. What travel modes do shared e-scooters displace? A review of recent research findings. Transp. Rev. 43 (1), 5–31.
Wang, T., Qu, Z., Yang, Z., Nichol, T., Clarke, G., Ge, Y.-E., 2020a. Climate change research on transportation systems: Climate risks, adaptation and planning. Transp. Res. D 88, 102553.
Wang, Y., Wu, J., Chen, K., Liu, P., 2021. Are shared electric scooters energy efficient? Commun. Transp. Res. 1, 100022.
Wang, Y., Xu, D., Peng, P., Xuan, Q., Zhang, G., 2020b. An urban commuters' OD hybrid prediction method based on big GPS data. Chaos 30 (9).
Xu, T., Han, G., Qi, X., Du, J., Lin, C., Shu, L., 2020a. A hybrid machine learning model for demand prediction of edge-computing-based bike-sharing system using Internet of Things. IEEE Internet Things J. 7 (8), 7345–7356.
Xu, C., Ji, J., Liu, P., 2018. The station-free sharing bike demand forecasting with a deep learning approach and large-scale datasets. Transp. Res. C 95, 47–60.
Xu, M., Liu, H., Yang, H., 2020b. A deep learning based multi-block hybrid model for bike-sharing supply-demand prediction. IEEE Access 8, 85826–85838.
Yan, X., Zhao, X., Broaddus, A., Johnson, J., Srinivasan, S., 2023. Evaluating shared e-scooters' potential to enhance public transit and reduce driving. Transp. Res. D 117, 103640.
Yang, Y., Heppenstall, A., Turner, A., Comber, A., 2020. Using graph structural information about flows to enhance short-term demand prediction in bike-sharing systems. Comput. Environ. Urban Syst. 83, 101521.
Yang, B., Tian, Y., Wang, J., Hu, X., An, S., 2022. How to improve urban transportation planning in big data era? A practice in the study of traffic analysis zone delineation. Transp. Policy 127, 1–14.
Yu, Y., Si, X., Hu, C., Zhang, J., 2019. A review of recurrent neural networks: LSTM cells and network architectures. Neural Comput. 31 (7), 1235–1270.
Zakhem, M., Smith-Colin, J., 2021. Micromobility implementation challenges and opportunities: Analysis of e-scooter parking and high-use corridors. Transp. Res. D 101, 103082.
Zeng, W., Lin, C., Liu, K., Lin, J., Tung, A.K., 2021. Modeling spatial nonstationarity via deformable convolutions for deep traffic flow prediction. IEEE Trans. Knowl. Data Eng..
Zhang, X., Zhao, X., 2022. Machine learning approach for spatial modeling of ridesourcing demand. J. Transp. Geogr. 100, 103310.
Zhao, P., Haitao, H., Li, A., Mansourian, A., 2021. Impact of data processing on deriving micro-mobility patterns from vehicle availability data. Transp. Res. D 97, 102913.
Zhou, J., 2022. Understanding and planning shared micro-mobility. Transp. Res. D 103, 103172.